

# Stable Fe isotope fractionations produced by aqueous Fe(II)-hematite surface interactions

Lingling Wu<sup>a,b,\*</sup>, Brian L. Beard<sup>a,b</sup>, Eric E. Roden<sup>a,b</sup>, Christopher B. Kennedy<sup>c</sup>,  
Clark M. Johnson<sup>a,b</sup>

<sup>a</sup> Department of Geoscience, University of Wisconsin–Madison, 1215 West Dayton Street, Madison, WI 53706, USA

<sup>b</sup> NASA Astrobiology Institute, University of Wisconsin–Madison, Madison, WI 53706, USA

<sup>c</sup> SRK Consulting, Suite 2100, 25 Adelaide St. East, Toronto, ON, M5C 3A1 Canada

Received 11 December 2009; accepted in revised form 26 April 2010; available online 6 May 2010

## Abstract

Stable Fe isotope fractionations were investigated during exposure of hematite to aqueous Fe(II) under conditions of variable Fe(II)/hematite ratios, the presence/absence of dissolved Si, and neutral versus alkaline pH. When Fe(II) undergoes electron transfer to hematite, Fe(II) is initially oxidized to Fe(III), and structural Fe(III) on the hematite surface is reduced to Fe(II). During this redox reaction, the newly formed reactive Fe(III) layer becomes enriched in heavy Fe isotopes and light Fe isotopes partition into aqueous and sorbed Fe(II). Our results indicate that in most cases the reactive Fe(III) that undergoes isotopic exchange accounts for less than one octahedral layer on the hematite surface. With higher Fe(II)/hematite molar ratios, and the presence of dissolved Si at alkaline pH, stable Fe isotope fractionations move away from those expected for equilibrium between aqueous Fe(II) and hematite, towards those expected for aqueous Fe(II) and goethite. These results point to formation of new phases on the hematite surface as a result of distortion of Fe–O bonds and Si polymerization at high pH. Our findings demonstrate how stable Fe isotope fractionations can be used to investigate changes in surface Fe phases during exposure of Fe(III) oxides to aqueous Fe(II) under different environmental conditions. These results confirm the coupled electron and atom exchange mechanism proposed to explain Fe isotope fractionation during dissimilatory iron reduction (DIR). Although abiogenic Fe(II)<sub>aq</sub>–oxide interaction will produce low  $\delta^{56}\text{Fe}$  values for Fe(II)<sub>aq</sub>, similar to that produced by Fe(II) oxidation, only small quantities of low- $\delta^{56}\text{Fe}$  Fe(II)<sub>aq</sub> are formed by these processes. In contrast, DIR, which continually exposes new surface Fe(III) atoms during reduction, as well as production of Fe(II), remains the most efficient mechanism for generating large quantities of low- $\delta^{56}\text{Fe}$  aqueous Fe(II) in many natural systems.

© 2010 Elsevier Ltd. All rights reserved.

## 1. INTRODUCTION

Iron oxides are an important component of the Fe cycle in surface environments, reflecting the end product of Fe(II) oxidation, as well as substrates for reductive processes. Redox transformations of iron play an important role in the fate and transport of natural and contaminant compounds

in soil and groundwater environments (Lovley, 1989; Heijman et al., 1995; Rügge et al., 1998). Under oxygen-limited conditions, dissimilatory iron-reducing bacteria produce Fe(II) through enzymatic reduction of Fe(III) oxide surfaces (Heijman et al., 1993; Fredrickson and Gorby, 1996). Aqueous Fe(II) in the presence of mineral surfaces has been shown to reduce and attenuate contaminants in the subsurface (e.g., Buerge and Hug, 1999; Liger et al., 1999; Pecher et al., 2002; Vikesland and Valentine, 2002; Hofstetter et al., 2003; Strathmann and Stone, 2003; Elsnor et al., 2004a,b).

Extensive literature exists on interaction of Fe(II) with oxide/hydroxide surfaces (e.g., Liger et al., 1999; Williams

\* Corresponding author at: Department of Geoscience, University of Wisconsin–Madison, 1215 West Dayton Street, Madison, WI 53706, USA. Tel.: +1 608 890 0929.

E-mail address: [lwu@geology.wisc.edu](mailto:lwu@geology.wisc.edu) (L. Wu).

and Scherer, 2004; Hiemstra and van Riemsdijk, 2007; Larese-Casanova and Scherer, 2007). Electron transfer during these abiotic interactions is well documented (e.g., Tronc et al., 1984; Williams and Scherer, 2004; Silvester et al., 2005; Kerisit and Rosso, 2006; Hiemstra and van Riemsdijk, 2007; Larese-Casanova and Scherer, 2007). Mössbauer spectroscopy has shown that at low Fe(II) concentrations, sorbed Fe(II) species undergo interfacial electron transfer and atom exchange with structural Fe(III) in hematite, and when Fe(II) concentrations exceed surface site saturation, a stable sorbed Fe(II) phase forms on the hematite surface (Williams and Scherer, 2004; Larese-Casanova and Scherer, 2007). Crystal truncation rod diffraction has provided indirect evidence for oxidation of adsorbed Fe(II) on hematite based on the observation that the Fe–O bond lengths of the surface Fe atoms are characteristic of Fe(III) (Tanwar et al., 2008, 2009). Isotopic tracer studies have documented significant atom exchange between aqueous Fe(II) and ferrihydrite and goethite, but limited exchange with hematite (e.g., Pedersen et al., 2005; Handler et al., 2009).

In this study, stable Fe isotope fractionations between Fe(II) and hematite are used to interrogate changes in the surface structure of hematite. In particular, we sought to test the coupled electron and atom exchange mechanism proposed to explain the Fe isotope fractionations produced by dissimilatory iron reduction (DIR) in previous studies (Crosby et al., 2005, 2007). A number of experimental studies have shown isotopically light aqueous Fe(II) relative to the initial Fe(III) substrate produced by DIR (Beard et al., 1999, 2003; Icopini et al., 2004; Crosby et al., 2005; Johnson et al., 2005; Crosby et al., 2007). Using acid extractions, Crosby et al. (2005) determined for the first time that the high  $^{56}\text{Fe}/^{54}\text{Fe}$  component required for isotopic mass balance was a reactive Fe(III) layer on the oxide surface (defined here as  $\text{Fe(III)}_{\text{reac}}$ ). The isotopic fractionations between aqueous Fe(II) and  $\text{Fe(III)}_{\text{reac}}$  during dissimilatory microbial reduction of hematite match those determined in equilibrium experiments (Skulan et al., 2002; Welch et al., 2003), and Crosby et al. (2005, 2007) interpreted this to reflect coupled electron and atom exchange between Fe(II) and the oxide surface, that was catalyzed by bacteria

through production of Fe(II). Moreover, Wu et al. (2009) noted distinct Fe isotope fractionations were produced by microbial hematite reduction as a function of pH and dissolved Si. Because Fe isotope fractionations fundamentally reflect the nature of Fe bonding, changes in isotopic fractionation can be used to monitor changes in Fe bonding in surface layers of hematite that accompany electron transfer between Fe(II) and hematite. In addition to determining the effect of pH, studying the effects of dissolved Si was a goal because this is a common species in warm groundwater systems and is known to inhibit contaminant reduction by reduced Fe species (Kohn et al., 2005; Mishra and Farrell, 2005; Reardon et al., 2008). Dissolved silica was also important in Precambrian marine systems prior to development of silica-secreting organisms (e.g., Maliva et al., 2005; Konhauser et al., 2007), and hence the potential influence of Si on Fe(II)–Fe(III) oxide isotope exchange may have important implications for interpretation of the Fe isotope record in Archean and Proterozoic rocks.

## 2. METHODS

### 2.1. Experimental design

Experiments were conducted with and without 2.14 mM Si ( $\text{Na}_2\text{SiO}_3 \cdot 9\text{H}_2\text{O}$ ) at pH 7 and pH 8.7 (see Table 1 for a summary of the experiments conducted). The reactors were either agitated once at the time of sampling, or agitated continuously on a tube roller. Hematite ( $\alpha\text{-Fe}_2\text{O}_3$ ) was purchased from Fisher Scientific (Naltham, MA, USA). This is the same hematite used in the DIR experiments of Wu et al. (2009). Particles were approximately spherical, had an average diameter of 100 nm, as determined by TEM, and had a BET surface area of 10.8  $\text{m}^2/\text{g}$ . Experiments were carried out in separate 20 mL serum glass bottles with 10 mL anoxic ( $\text{N}_2$ -bubbled) Pipes buffer (10 mM) with or without 2.14 mM Si, containing 50 mmol/L of hematite. An exception is experiment 1C, where the effects of variable molar Fe(II)/hematite ratios on the measured isotopic fractionations were tested. The experiments were initiated by addition of  $\text{FeCl}_2$  from an anaerobic stock solution. All

Table 1  
Summary of experiments.

Experiment	Description <sup>a</sup>	Data table <sup>b</sup>
1A	pH 7, no Si, 1× agitation	EA1
1B	pH 7, no Si, constant agitation	EA2
1C	pH 7, no Si, constant agitation, variable Fe(II)/hematite ratios	EA3
2A	pH 7, Si added, 1× agitation	EA4
2B	pH 7, Si added, constant agitation	EA5
3A	pH 8.7, no Si, 1× agitation	EA6
3B	pH 8.7, no Si, constant agitation	EA7
4A	pH 8.7, Si added, 1× agitation	EA8
4B	pH 8.7, Si added, constant agitation	EA9
Controls	No hematite at pH 7 and 8.7, with and without Si, 1× and constant agitation	EA10

<sup>a</sup> Fe(II)/hematite ratio is 0.5/50 mM for all experiments except experiment 1C where Fe(II)/hematite ratios are variable. “1× agitation” denotes that the reactor was agitated once at the time of sampling, and “constant agitation” denotes that the reactor was constantly agitated on a roller tube.

<sup>b</sup> Data tables are presented in electronic annexes.

Table 2  
Summary of operational terms.

Term	Description	Quantity	Isotopic composition
Fe(II) <sub>aq</sub>	Aqueous Fe(II)	Measured	Measured
Fe(II) <sub>sorb</sub> (0.05 M HCl) = 0.05 M HCl extract	Sorbed Fe(II) extracted by 0.05 M HCl	Measured	Measured
Fe(II) <sub>sorb</sub> (0.5 M HCl)	Sorbed Fe(II) extracted by 0.5 M HCl	Measured	Assumed to be equal to that of Fe(II) <sub>sorb</sub> (0.05 M HCl)
Fe(II) <sub>sorb</sub>	Sum of Fe(II) <sub>sorb</sub> (0.05 M HCl) and Fe(II) <sub>sorb</sub> (0.5 M HCl)	Calculated	Assumed to be equal to that of Fe(II) <sub>sorb</sub> (0.05 M HCl)
Fe <sub>HCl</sub> = 0.5 M HCl extract	Fe extracted by 0.5 M HCl A mixture of part of Fe(III) <sub>react</sub> and Fe(II) <sub>sorb</sub> (0.5 M HCl)	Measured	Measured
Fe(III) <sub>react</sub>	Reactive Fe(III) layer on hematite surface	Calculated	Calculated
Fe(II) in hematite	Fe(II) in bulk dissolution of hematite by 1 M HCl	Measured	Assumed to be equal to bulk hematite

sampling was carried out in an anaerobic chamber (Coy Products, Grass Lake, MI, USA). A parallel set of hematite-free control experiments was conducted under identical conditions, which confirmed maintenance of anaerobic conditions.

## 2.2. Fe phase separation and wet chemical analysis

Table 2 contains a summary of the operational terms relevant to the Fe phases analyzed for bulk concentration and isotope composition. Bottles containing 10 mL aliquots of the reaction slurries were centrifuged to remove the aqueous fraction (Fe(II)<sub>aq</sub>) after 8, 13, and 20 days for all experiments, except experiment 1C (see Table 1), where samples were taken after 4, 8, and 12 days. The remaining solids were leached for 10 min using 0.05 M HCl, which removed the majority of sorbed Fe(II) (Fe(II)<sub>sorb</sub>) without dissolving any underlying Fe(III), as was confirmed by Fe(II) and total Fe measurements. Fe(II) and total Fe concentrations were measured using *Ferrozine* (Stokey, 1970), and Fe(III) was determined by difference. The Fe concentrations were measured three times for each sample and the error is within 3%. A second extraction using 0.5 M HCl for one hour dissolved a small amount of ferric oxide based on trial tests, and this presumably reflects the most reactive part of the hematite crystals. This reactive fraction is referred to as “Fe(III)<sub>react</sub>” for purposes of Fe isotope fractionation and mass-balance calculations (see Section 3.2; Table 2), the same usage we followed in our previous studies (Crosby et al., 2005, 2007; Wu et al., 2009). The 0.5 M HCl extraction also dissolved any remaining sorbed Fe(II). Total Fe(II)<sub>sorb</sub> is defined as the sum of Fe(II)<sub>sorb</sub> (0.05 M HCl) and Fe(II)<sub>sorb</sub> (0.5 M HCl) (Table 2). In order to obtain high proportions of Fe(III) in the 0.5 M HCl extract, extraction time was extended to 18 h for later time point samples.

Complete recovery of Fe(II) (101 ± 12%) was achieved by measuring Fe(II) that partitioned into the hematite and was not recoverable with 0.5 M HCl. This effect has been noted by other studies of Fe(II)<sub>aq</sub>-iron oxide interactions (e.g., Jeon et al., 2003; Williams and Scherer, 2004; Larese-Casanova and Scherer, 2007). Remaining hematite was dissolved using 1 M HCl at 70 °C and Fe(II) in hema-

tite was measured using NH<sub>4</sub>F to mask the influence of Fe(III) on the absorption spectra (Krishnamurti and Huang, 1990). No Fe(II) was detected in pure hematite that was not exposed to Fe(II), using two sequential extractions with the same method. All samples were passed through 0.2 µm filters, and aqueous and the 0.05 M HCl fractions were acidified with HCl. Silica concentrations in aqueous phase samples and HCl extracts were measured by ICP-OES.

For hematite-free control experiments, aqueous samples were quantitatively recovered for all of the pH 7 experiments. A white Fe(II)-Si gel formed in all of the pH 8.7 plus Si experiments, and mixed-valence green rust formed in the pH 8.7 no Si experiments that were agitated once; green rust was not observed for the experiments that were constantly agitated. Samples were centrifuged to separate Fe(II)-Si gel or green rust from the aqueous fraction, and the supernatant was passed through a 0.2 µm filter. The Fe-Si gel or green rust pellet was removed using a pipette and dissolved using 0.5 M HCl. 1 mL of 0.5 M HCl was then added to the bottle in order to retrieve the residue attached to the bottle wall. Finally, the filter paper was collected and dissolved in 7 M HCl to completely recover added Fe for the pH 8.7 plus Si control experiments. Concentrations of Fe and Si in different fractions were measured, as described above.

## 2.3. Fe isotope measurements and nomenclature

All Fe(II)<sub>aq</sub>, 0.05 M HCl, and 0.5 M HCl fractions were purified using anion-exchange chromatography, followed by Fe isotope measurements using a MC-ICP-MS, as previously described (Beard et al., 2003). The isotopic composition of Fe(II) contained in hematite could not be measured due to the small amount of Fe(II) relative to the large amount of Fe(III) in hematite. Data are reported as <sup>56</sup>Fe/<sup>54</sup>Fe ratios relative to the average of igneous rocks, in standard δ notation:

$$\delta^{56}\text{Fe} = \left[ \frac{{}^{56}\text{Fe}/{}^{54}\text{Fe}_{\text{sample}}}{{}^{56}\text{Fe}/{}^{54}\text{Fe}_{\text{std}}} - 1 \right] \times 10^3 \quad (1)$$

where <sup>56</sup>Fe/<sup>54</sup>Fe<sub>std</sub> is the average of igneous rocks. δ<sup>57</sup>Fe values may be defined in an analogous manner using the <sup>57</sup>Fe/<sup>54</sup>Fe ratio, and because natural Fe sources were used,

$\delta^{57}\text{Fe}$  and  $\delta^{56}\text{Fe}$  values are related in a mass-dependent manner. Measured external precision in  $\delta^{56}\text{Fe}$  values is  $\pm 0.08\text{‰}$  ( $2\sigma$ ) based on replicate standard analyses ( $n = 112$ ). For  $\text{Fe(II)}_{\text{aq}}$  in pH 8.7 plus Si experiments, where Fe contents were less than 15  $\mu\text{g}$ , the precision in  $\delta^{56}\text{Fe}$  values is conservatively estimated as  $\pm 0.16\text{‰}$  ( $2\sigma$ ). On the igneous rock scale, the  $\delta^{56}\text{Fe}$  value of the IRMM-014 standard is  $-0.09\text{‰}$  (Beard et al., 2003). Partial dissolution tests show that the initial  $\delta^{56}\text{Fe}$  value of the hematite was  $+0.13\text{‰}$ , and that the hematite is isotopically homogenous within analytical uncertainty (Wu et al., 2009). The initial  $\delta^{56}\text{Fe}$  value of  $\text{FeCl}_2$  was  $-0.52\text{‰} \pm 0.05\text{‰}$  ( $2\sigma$ ;  $n = 28$ ).

Stable Fe isotope fractionation between two components A and B are described as

$$\alpha_{A-B}^{56} = \frac{{}^{56}\text{Fe}/{}^{54}\text{Fe}_A}{{}^{56}\text{Fe}/{}^{54}\text{Fe}_B} \quad (2)$$

following standard practice. Under equilibrium conditions,  $\alpha_{A-B}^{56}$  reflects fundamental differences in the thermodynamic properties of components A and B, which may be related to differences in the molecular partition functions through classical statistical thermodynamics (see recent review in Schauble, 2004). To a very good approximation,  $\alpha_{A-B}^{56}$

may be related to differences in the  $\delta^{56}\text{Fe}$  values through the relation:

$$\Delta^{56}\text{Fe}_{A-B} = \delta^{56}\text{Fe}_A - \delta^{56}\text{Fe}_B \approx 10^3 \ln \alpha_{A-B}^{56} \quad (3)$$

### 3. RESULTS

#### 3.1. Proportions and isotopic compositions of components that underwent atom exchange

The proportions of aqueous  $\text{Fe(II)}$  and 0.05 M HCl-extractable  $\text{Fe(II)}_{\text{sorb}}$  were relatively constant with time at pH 7, regardless of the presence or absence of Si and agitation times, although the proportions of these components were a function of the total  $\text{Fe(II)}$ /hematite ratios of specific experiments (Fig. 1, electronic annex Tables EA1–5). The proportion of  $\text{Fe(II)}_{\text{aq}}$  was much smaller at pH 8.7 (Fig. 2, Tables EA6–9), and  $\text{Fe(II)}_{\text{sorb}}$  extracted using 0.05 M HCl was the major component of total  $\text{Fe(II)}$ , an observation that was not affected by presence or absence of Si and agitation times. Sorption of  $\text{Fe(II)}$  onto hematite was  $\sim 35\%$  and  $\sim 70\%$  in pH 7 and pH 8.7 experiments, respectively, which is consistent with increased sorption of

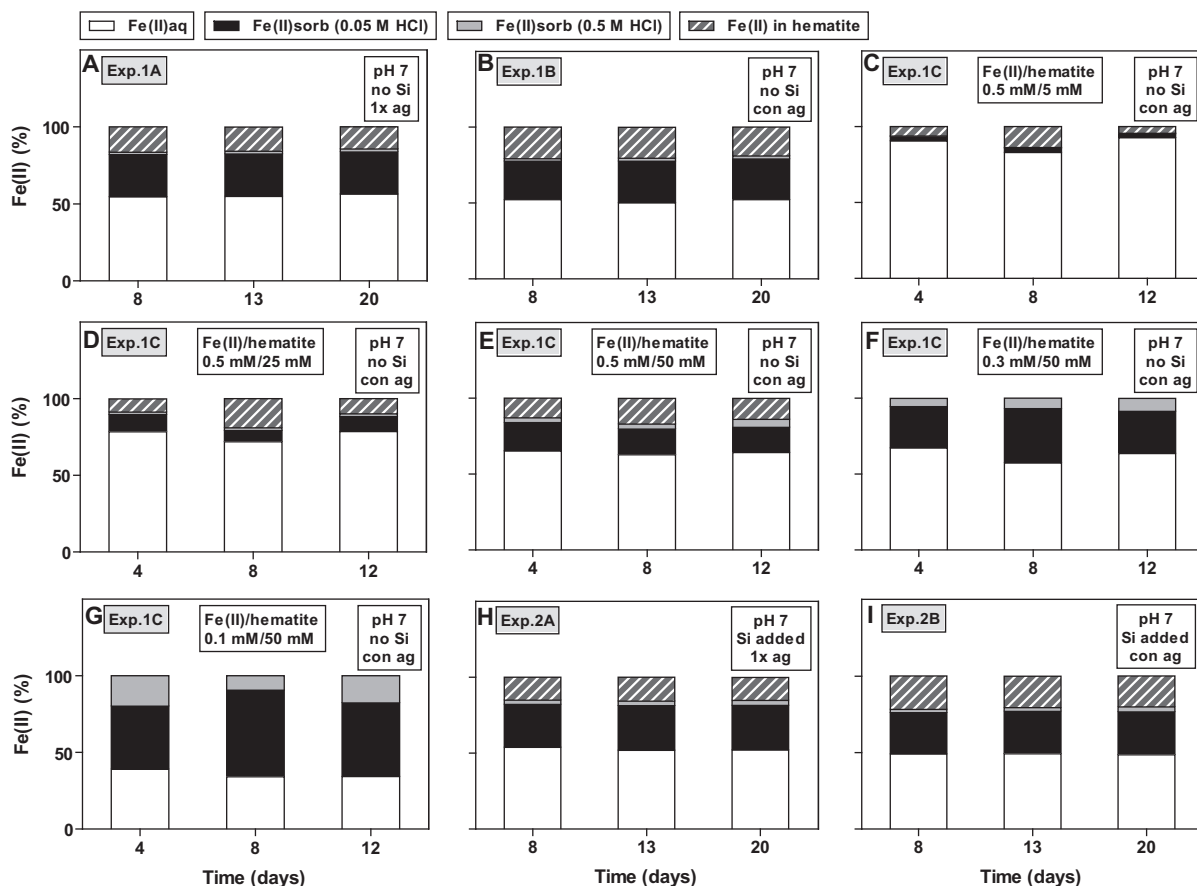


Fig. 1. Proportions of aqueous  $\text{Fe(II)}$ , sorbed  $\text{Fe(II)}$  in the 0.05 M HCl extract and 0.5 M HCl extract, and  $\text{Fe(II)}$  in hematite during interactions between  $\text{Fe(II)}$  and hematite at pH 7 in the absence of dissolved Si agitated once during sampling (A), constantly agitated (B), and constantly agitated with variable  $\text{Fe(II)}$ /hematite ratios (C–G) and in the presence of Si (2.14 mM Si) agitated once during sampling (H) and constantly agitated (I).  $\text{Fe(II)}$ /hematite ratio was 0.5 mM/50 mM for experiment 1A, 1B, 2A and 2B. See tables EA1–5 for errors from duplicate suspensions. Note that the proportion of sorbed  $\text{Fe(II)}$  in the 0.5 M HCl extract is very small compared with other phases.

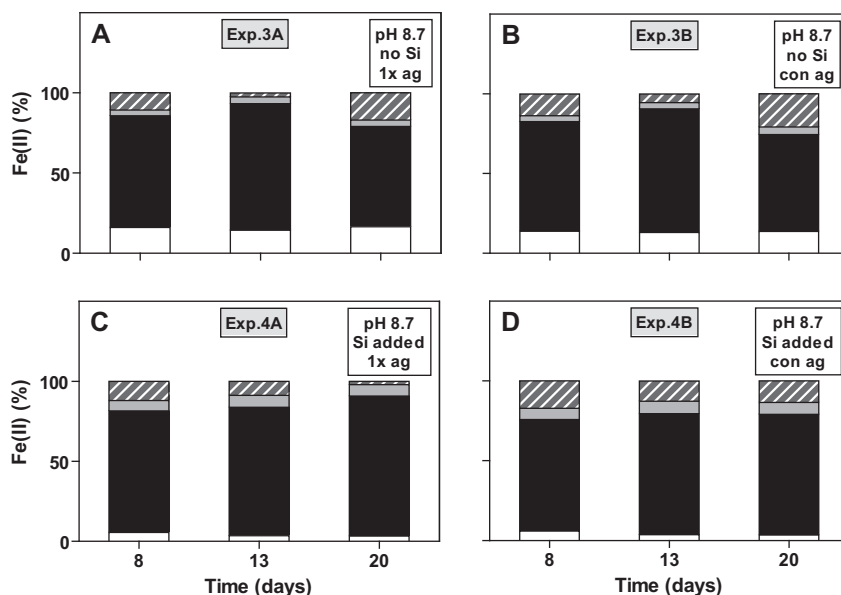


Fig. 2. Proportions of aqueous Fe(II), sorbed Fe(II) in the 0.05 M HCl extract and 0.5 M HCl extract, and Fe(II) in hematite during interactions between Fe(II) and hematite at pH 8.7 in the absence of dissolved Si agitated once during sampling (A), constantly agitated (B), and in the presence of Si (2.14 mM Si) agitated once during sampling (C) and constantly agitated (D). Symbols are identical to Fig. 1. See tables EA6-9 for errors from duplicate suspensions.

Fe(II) to hematite surfaces when pH is increased (e.g., Liger et al., 1999; Jeon et al., 2001; Strathmann and Stone, 2003). The sum of aqueous Si, and Si in 0.05 M HCl and 0.5 M HCl extracts, was essentially equal to the amount added, within analytical error (Fig. EA1, Tables EA4, 5, 8 and 9), suggesting no silica was precipitated in these experiments. The 0.05 M HCl extraction recovered exclusively Fe(II), whereas 0.5 M HCl extractions removed a mixture of Fe(II) and Fe(III).

A minor fraction of Fe(II) was incorporated into the hematite structure ( $\sim 20\%$  and  $\sim 10\%$  of added Fe(II) in pH 7 and 8.7 experiments, respectively; Figs. 1 and 2, Tables EA1–9), and could be recovered only through complete dissolution of the mineral by heating in 1 M HCl. The apparently irreversible incorporation of reducing equivalents into the hematite structure is consistent with other reports of incomplete recovery of added Fe(II) by acidification with weak (0.5 M) HCl at room temperature (e.g., Jeon et al., 2003; Williams and Scherer, 2004; Larese-Casanova and Scherer, 2007). Because the Fe(II) incorporated in hematite reflects electron transfer to the interior of the crystals (Kerisit and Rosso, 2006, 2007), and not transfer of atoms, no Fe isotope effects are anticipated. The Fe(II) in the interior of the hematite crystals could only undergo isotopic exchange with the solution if solid-state diffusion occurred on the timescales of the experiments, which is not possible at the low temperature used in this study. For the hematite-free control experiments, added Fe(II) existed exclusively as Fe(II)<sub>aq</sub> at pH 7 (Table EA10). At pH 8.7, a large proportion of Fe(II) formed Fe–Si gel in plus Si experiments and green rust in the no Si experiments (Fig. EA2, Table EA10).

The Fe isotope composition of Fe(II)<sub>aq</sub> is measured directly, and the isotopic composition of Fe(II)<sub>sorb</sub> is obtained from the 0.05 M HCl extraction. That these isotopic com-

positions do not match those of the starting FeCl<sub>2</sub> clearly indicates that atom exchange occurred (Figs. 3 and 4). As noted by Crosby et al. (2005, 2007) and Wu et al. (2009), determination of the Fe isotope composition of Fe(III) sampled in the 0.5 M HCl extraction ( $\delta^{56}\text{Fe}_{\text{Fe(III)react}}$ ) requires “unmixing” the Fe(II) and Fe(III) components (Figs. 5 and EA3). To do this,  $\delta^{56}\text{Fe}$  values of the Fe(II) component were assumed to be the same as Fe(II)<sub>sorb</sub> recovered by the 0.05 M HCl extraction; this assumption is supported by the observation of consistent isotopic fractionations over a range of Fe(II)<sub>aq</sub> and Fe(II)<sub>sorb</sub> contents (Crosby et al., 2007; Wu et al., 2009).

The  $\delta^{56}\text{Fe}$  value for Fe(III)<sub>react</sub> is calculated by extrapolating from the  $\delta^{56}\text{Fe}$  value for Fe(II)<sub>sorb</sub>, through the measured  $\delta^{56}\text{Fe}$  value of the 0.5 M HCl extraction to the intercept at  $X_{\text{Fe(II)}} = 0$  (Fig. 5). The most precise estimates of  $\delta^{56}\text{Fe}_{\text{Fe(III)react}}$  are obtained for 0.5 M HCl extracts that have high proportions of Fe(III). The 0.5 M HCl extracts of the pH 7 no Si experiments contained Fe(III)/total Fe ratios greater than 0.8, compared with Fe(III)/total Fe ratios of  $\sim 0.4$  in the pH 7 Si added experiments (Tables EA1–5). Most of the 0.5 M HCl extracts of the pH 8.7 experiments, except for those from the initial time point, were predominately composed of Fe(III), with Fe(III)/total Fe ratios  $> 0.6$  (Tables EA6–9). The  $2\sigma$  errors for  $\delta^{56}\text{Fe}_{\text{Fe(III)react}}$  were propagated from uncertainties for  $X_{\text{Fe(II)}}$  and  $\delta^{56}\text{Fe}$  values of Fe(II)<sub>sorb</sub> and 0.5 M HCl extract using ISOPLOT (Ludwig, 1991) and were mostly  $< 0.4\text{‰}$  for extracts with  $< 60\%$  Fe(III) and  $< 0.2\text{‰}$  for extracts with  $> 60\%$  Fe(III). Calculated  $\delta^{56}\text{Fe}_{\text{Fe(III)react}}$  values for the no Si experiments were  $+1.1\text{‰}$  at pH 7, and ranged from  $+1.1$  to  $+1.6\text{‰}$  at pH 8.7 (Figs. 3 and 4). For the Si added experiments, the  $\delta^{56}\text{Fe}_{\text{Fe(III)react}}$  values ranged from  $+1.0$  to  $+2.0\text{‰}$  at pH 7, and  $+0.8$  to  $+2.5\text{‰}$  at pH 8.7.

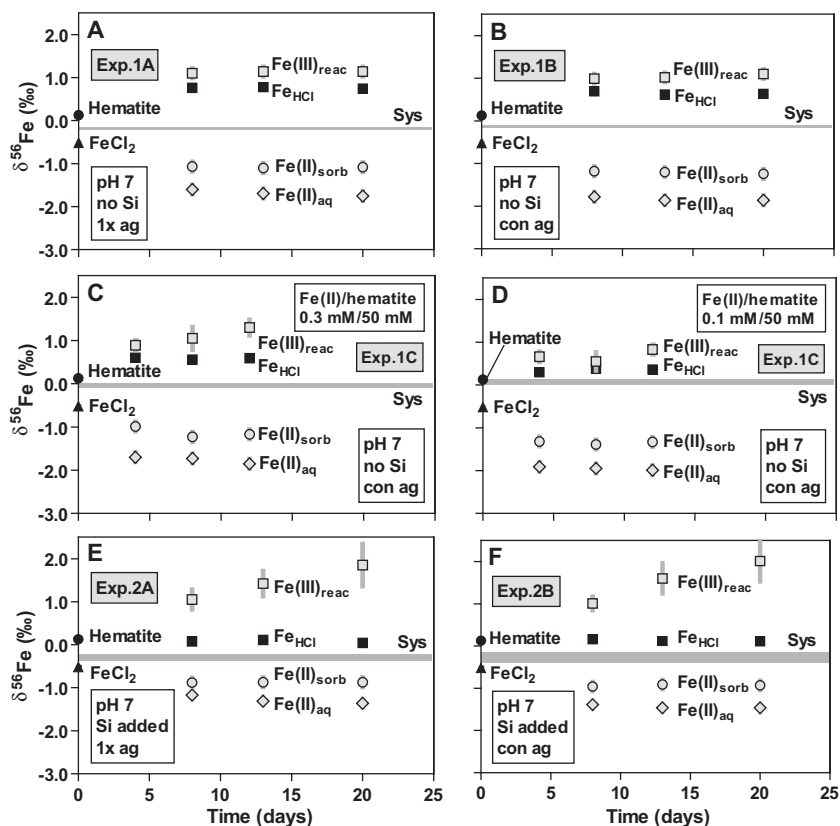


Fig. 3. Temporal changes in measured  $\delta^{56}\text{Fe}$  values for aqueous Fe(II) ( $\text{Fe(II)}_{\text{aq}}$ ), sorbed Fe(II) in the 0.05 M HCl extract ( $\text{Fe(II)}_{\text{sorb}}$ ), and total Fe (both Fe(II) and Fe(III)) in the 0.5 M HCl extract ( $\text{Fe}_{\text{HCl}}$ ), and calculated  $\delta^{56}\text{Fe}$  values for reactive Fe(III) component at hematite surface ( $\text{Fe(III)}_{\text{reac}}$ ) at pH 7 experiments. The gray horizontal bars show the system Fe isotope composition. The width of bars is based on  $\pm 2\sigma$  uncertainty from multiple time points for each experiment. The isotopic compositions for starting hematite and  $\text{FeCl}_2$  are shown by dark circle and triangle, respectively.

The uncertainties in the calculated  $\delta^{56}\text{Fe}$  values for  $\text{Fe(III)}_{\text{reac}}$  directly reflect the extent of extrapolation to  $X_{\text{Fe(II)}} = 0$  in Fig. 5, where the proportion of Fe(II) in the 0.5 M HCl extraction is high, the differences will be largest between the measured  $\delta^{56}\text{Fe}$  values in the 0.5 M HCl extraction and the calculated  $\delta^{56}\text{Fe}$  value for  $\text{Fe(III)}_{\text{reac}}$ , and this will be correlated with a relatively high uncertainty for the Fe isotope composition of  $\text{Fe(III)}_{\text{reac}}$ . This relation can be clearly seen, for example, in Fig. 3E and F, as well as Fig. 4C and D, where relatively high uncertainties for the  $\delta^{56}\text{Fe}$  values of  $\text{Fe(III)}_{\text{reac}}$  are associated with samples that have the largest extrapolation from the  $\delta^{56}\text{Fe}$  values of the 0.5 M HCl extraction. As discussed below, the uncertainties in  $\delta^{56}\text{Fe}_{\text{Fe(III)reac}}$  are propagated to the uncertainties in the isotopic fractionation factor ( $\alpha_{\text{A-B}}^{56}$  or  $\Delta^{56}\text{Fe}_{\text{A-B}}$ ).

### 3.2. Abundances of components in the total reactive Fe pool

The proportions of Fe components that underwent isotopic exchange during  $\text{Fe(II)}_{\text{aq}}$ -hematite interaction may be calculated using an isotopic mass-balance equation (Crosby et al., 2007; Wu et al., 2009). The mole sum of  $\text{Fe(II)}_{\text{aq}}$ ,  $\text{Fe(II)}_{\text{sorb}}$ , and  $\text{Fe(III)}_{\text{reac}}$  is defined as the total reactive Fe pool ( $M_{\text{TOT ReacFe}}$ ) that underwent isotopic exchange, and this pool must have the same isotopic composition as the starting system, as described by the following equation:

$$\begin{aligned} \delta^{56}\text{Fe}_{\text{Sys}} \cdot M_{\text{TOT ReacFe}} &= \delta^{56}\text{Fe}_{\text{FeCl}_2} \cdot (M_{\text{Fe(II)aq}} + M_{\text{Fe(II)sorb}}) \\ &\quad + \delta^{56}\text{Fe}_{\text{Hem}} \cdot M_{\text{Fe(III)reac}} \\ &= \delta^{56}\text{Fe}_{\text{Fe(II)aq}} \cdot M_{\text{Fe(II)aq}} \\ &\quad + \delta^{56}\text{Fe}_{\text{Fe(II)sorb}} \cdot M_{\text{Fe(II)sorb}} \\ &\quad + \delta^{56}\text{Fe}_{\text{Fe(III)reac}} \cdot M_{\text{Fe(III)reac}} \end{aligned} \quad (4)$$

The Fe(II) incorporated into the hematite was excluded from Eq. (4) because the Fe(II) atoms in bulk hematite are the product of *in situ* reduction of structural Fe(III) via electron addition, and therefore, as noted above, could not have undergone atom exchange with Fe(III) on the surface. Evidence for conversion of Fe(III) to Fe(II) within hematite lies in work which has demonstrated that electrons readily delocalize and rapidly diffuse away from the initial site of interfacial electron transfer to the interior of the hematite lattice (Kerisit and Rosso, 2006, 2007).

In our experiments, the moles of  $\text{Fe(II)}_{\text{aq}}$  ( $M_{\text{Fe(II)aq}}$ ) are determined by the measured concentrations and the volume of  $\text{Fe(II)}_{\text{aq}}$ . The moles of  $\text{Fe(II)}_{\text{sorb}}$  ( $M_{\text{Fe(II)sorb}}$ ) are the sum of Fe(II) measured in the 0.05 M HCl and 0.5 M HCl extracts. The moles of  $\text{Fe(III)}_{\text{reac}}$  ( $M_{\text{Fe(III)reac}}$ ) cannot be directly measured but can be calculated based on the above isotopic mass balance expression. Solving Eq. (4) for  $M_{\text{Fe(III)reac}}$  produces:

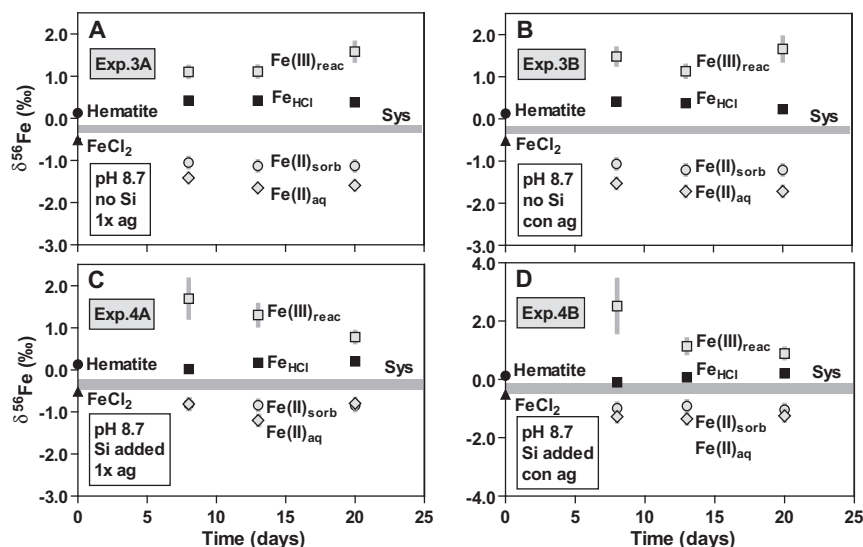


Fig. 4. Temporal changes in measured  $\delta^{56}\text{Fe}$  values for  $\text{Fe(II)}_{\text{aq}}$ ,  $\text{Fe(II)}_{\text{sorb}}$ , and  $\text{Fe}_{\text{HCl}}$ , and calculated  $\delta^{56}\text{Fe}$  values for  $\text{Fe(III)}_{\text{reac}}$  at pH 8.7 experiments. The gray horizontal bars show the system Fe isotope composition. The width of bars is based on  $\pm 2\sigma$  uncertainty from multiple time points for each experiment. The isotopic compositions for starting hematite and  $\text{FeCl}_2$  are shown by dark circle and triangle, respectively.

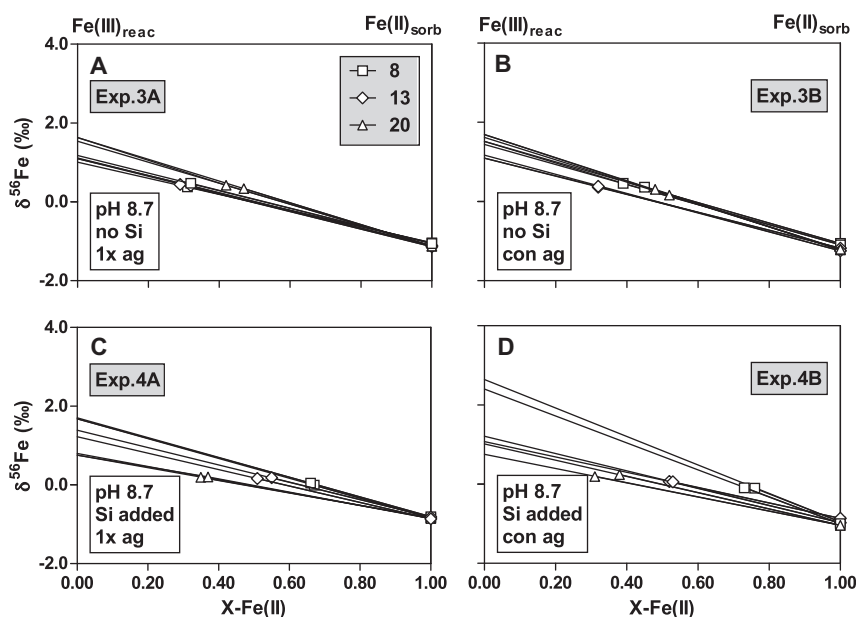


Fig. 5. Mixing diagrams illustrating calculation of Fe(III) end-member component in the 0.5 M HCl extracts, which contained mixtures of Fe(II) and Fe(III) for pH 8.7 experiments.

$$M_{\text{Fe(III)reac}} = \frac{\delta^{56}\text{Fe}_{\text{FeCl}_2} \cdot (M_{\text{Fe(II)aq}} + M_{\text{Fe(II)sorb}}) - \delta^{56}\text{Fe}_{\text{Fe(II)aq}} \cdot M_{\text{Fe(II)aq}} - \delta^{56}\text{Fe}_{\text{Fe(II)sorb}} \cdot M_{\text{Fe(II)sorb}}}{\delta^{56}\text{Fe}_{\text{Fe(III)reac}} - \delta^{56}\text{Fe}_{\text{Hem}}} \quad (5)$$

It is important to emphasize that  $M_{\text{Fe(III)reac}}$  is the amount of Fe(III) in hematite required to attain isotopic mass balance among  $\text{Fe(II)}_{\text{aq}}$ ,  $\text{Fe(II)}_{\text{sorb}}$ , and  $\text{Fe(III)}_{\text{reac}}$ , and this is not the same as the measured Fe(III) in the 0.5 M HCl extract. Calculated  $M_{\text{Fe(III)reac}}$  values were always greater than the measured Fe(III) content in the

0.5 M HCl extract; this, in fact, was an important goal in our experimental design, because if the moles of measured Fe(III) is less than  $M_{\text{Fe(III)reac}}$ , the likelihood of dissolving unreacted hematite during extraction is low. Embedded in Eq. (5) is the assumption that the calculated  $\delta^{56}\text{Fe}_{\text{Fe(III)reac}}$  in 0.5 M HCl extract is representative of the isotope

composition of total  $\text{Fe(III)}_{\text{reac}}$ . This assumption is supported by previous work that showed no isotopic fractionation occurs during proton-promoted dissolution of hematite using HCl (Skulan et al., 2002; Beard et al., 2003; Wu et al., 2009). The  $\delta^{56}\text{Fe}_{\text{Sys}}$  values calculated for each experiment, based on the molar proportions of Fe(II) and hematite added in each experiment, ranged from  $-0.2$  to  $-0.4\text{‰}$ . In order to make direct comparisons with previous isotopic studies, the data for each experiment were normalized to a system Fe isotope composition of  $\delta^{56}\text{Fe}_{\text{Sys}} = 0$ .

Increased pH generally reduced the amount of  $\text{Fe(III)}_{\text{reac}}$ , as well as the size of the total reactive Fe pool, regardless of the presence of Si (Table 3, Fig. EA4). The size of the reactive Fe pool did not significantly change over time in the no Si experiment, regardless of pH and agitation times. In the pH 7 plus Si experiment, the total amount of reactive Fe decreased from day 8 to day 13 and then leveled off. In the pH 8.7 plus Si experiment, the size of the reactive Fe pool increased gradually from day 8 to day 20. The relative proportions of  $\text{Fe(II)}_{\text{aq}}$ ,  $\text{Fe(II)}_{\text{sorb}}$ , and  $\text{Fe(III)}_{\text{reac}}$  ( $X_{\text{Fe(II)aq}}$ ,  $X_{\text{Fe(II)sorb}}$ ,  $X_{\text{Fe(III)reac}}$ ) did not change significantly with time at pH 7, regardless of the presence of Si and agitation times (Table 3, Fig. EA4). These components also remained relatively constant over time at pH 8.7 in the absence of Si. In contrast, the proportions of  $\text{Fe(II)}_{\text{aq}}$ ,  $\text{Fe(II)}_{\text{sorb}}$ , and  $\text{Fe(III)}_{\text{reac}}$  changed significantly over time at pH 8.7 in the presence of Si.  $X_{\text{Fe(III)reac}}$  increased over time, accompanied by complementary variations in  $X_{\text{Fe(II)sorb}}$  and  $X_{\text{Fe(II)aq}}$ .

#### 4. DISCUSSION

When Fe(II) undergoes electron exchange with hematite, Fe(II) is oxidized to Fe(III) and incorporated into hematite, and structural Fe(III) in hematite is reduced to Fe(II) that is released to the solution. Because Fe–O bond lengths change significantly when redox reactions occur (Eggleston et al., 2003; Tanwar et al., 2008), isotopic exchange should produce newly formed  $\text{Fe(III)}_{\text{reac}}$  that becomes enriched in heavy isotopes, and  $\text{Fe(II)}_{\text{aq}}$  and  $\text{Fe(II)}_{\text{sorb}}$  that become enriched in light isotopes (Crosby et al., 2005, 2007). The changes in Fe isotope compositions of  $\text{Fe(II)}_{\text{aq}}$ ,  $\text{Fe(II)}_{\text{sorb}}$ , and  $\text{Fe(III)}_{\text{reac}}$ , relative to the initial  $\delta^{56}\text{Fe}$  values for hematite and  $\text{FeCl}_2$ , provide clear evidence for such isotopic exchange. Below, we first discuss the isotopic fractionations among these components and compare them to those expected for the system  $\text{Fe(II)}_{\text{aq}}$ -hematite based on independent prior studies. Next we discuss the effects of pH and dissolved Si on the Fe isotope fractionations, which provide insights into the bonding environments of surface Fe(III). Finally, we address the implications for using Fe isotopes to trace biogeochemical cycling in nature.

##### 4.1. Isotopic fractionations among $\text{Fe(II)}_{\text{aq}}$ - $\text{Fe(II)}_{\text{sorb}}$ - $\text{Fe(III)}_{\text{reac}}$

The stable isotope fractionation between  $\text{Fe(II)}_{\text{aq}}$  and  $\text{Fe(II)}_{\text{sorb}}$ , defined as  $\Delta^{56}\text{Fe}_{\text{Fe(II)aq-Fe(II)sorb}}$ , was relatively invariant at  $-0.49 \pm 0.15\text{‰}$  throughout all experimental conditions (Figs. 6 and 7). This fractionation is similar to those obtained in dissimilatory iron reduction experiments, which obtained  $\delta^{56}\text{Fe}_{\text{Fe(II)aq-Fe(II)sorb}} = -0.30 \pm 0.08\text{‰}$

(Crosby et al., 2007), and  $-0.49 \pm 0.09\text{‰}$  (Wu et al., 2009), and suggests that isotopic equilibrium was obtained between  $\text{Fe(II)}_{\text{aq}}$  and  $\text{Fe(II)}_{\text{sorb}}$ . In contrast, the Fe isotope fractionation between  $\text{Fe(II)}_{\text{aq}}$  and reactive  $\text{Fe(III)}_{\text{reac}}$ , defined as  $\Delta^{56}\text{Fe}_{\text{Fe(II)aq-Fe(III)reac}}$ , varied depending upon experimental conditions.  $\Delta^{56}\text{Fe}_{\text{Fe(II)aq-Fe(III)reac}}$  changed little with time in the pH 7 no Si experiments, whereas in the pH 7 Si added experiments, it decreased from  $-2.22 \pm 0.24\text{‰}$  at day 8 to  $-3.21 \pm 0.50\text{‰}$  at day 20 when agitated once (Fig. 6), and from  $-2.40 \pm 0.18\text{‰}$  at day 8 to  $-3.49 \pm 0.49\text{‰}$  at day 20 when agitated constantly (Fig. 6). In the pH 8.7 no Si experiments,  $\Delta^{56}\text{Fe}_{\text{Fe(II)aq-Fe(III)reac}}$  also decreased similarly regardless of agitation times (Fig. 7).

The measured  $\Delta^{56}\text{Fe}_{\text{Fe(II)aq-Fe(III)reac}}$  fractionations determined at pH 7, without Si, can be directly compared to the experimentally determined  $\text{Fe(II)}_{\text{aq}}$ -hematite fractionations obtained by combining the studies of Skulan et al. (2002) and Welch et al. (2003), which produce  $\Delta^{56}\text{Fe}_{\text{Fe(II)aq-hem}} = -3.1\text{‰}$  at room temperature. Calculated  $\text{Fe(II)}_{\text{aq}}$ -hematite fractionations range from  $-0.2$  to  $-3.0\text{‰}$ , using the predicted fractionation factors based on spectroscopic data or *ab initio* calculations (Anbar et al., 2005; Blanchard et al., 2009; Ottonello and Zuccolini, 2009), but it is now recognized that there may be a systematic offset in predicted Fe isotope fractionations for aqueous species and minerals (Blanchard et al., 2009; Beard et al., 2010). We therefore prefer the experimentally determined  $\text{Fe(II)}_{\text{aq}}$ -hematite fractionation factors even if this is obtained through combining two separate experiments. At pH 7, in the absence of Si, the measured  $\Delta^{56}\text{Fe}_{\text{Fe(II)aq-Fe(III)reac}}$  fractionations (Fig. 6A and B) lie essentially within the  $0.3\text{‰}$  uncertainty of the experimentally determined equilibrium value. The initial isotopic contrast between the  $\text{FeCl}_2$  and hematite (prior to mixing) is  $-0.65\text{‰}$  ( $\delta^{56}\text{Fe}_{\text{FeCl}_2} = -0.52\text{‰}$ ,  $\delta^{56}\text{Fe}_{\text{hem}} = +0.13\text{‰}$ ), and the fact that, after mixing, the  $\text{Fe(II)}_{\text{aq}}$ - $\text{Fe(III)}_{\text{reac}}$  fractionation attained a value of  $-2.81 \pm 0.12\text{‰}$  ( $1 \times$  agitation) and  $-2.87 \pm 0.19\text{‰}$  (constant agitation) suggests that the hematite-bound Fe(III) sampled by the 0.5 M HCl extraction underwent equilibrium isotope exchange. These results provide confirmation that the mechanism of coupled electron transfer and atom exchange proposed by Crosby et al. (2005, 2007) between  $\text{Fe(II)}_{\text{aq}}$  and  $\text{Fe(III)}_{\text{reac}}$  is responsible for producing Fe isotope fractionations during DIR. Moreover, our results confirm the proposal of Crosby et al. (2007) that the Fe isotope fractionations produced between  $\text{Fe(II)}_{\text{aq}}$  and hematite are fundamentally equilibrium fractionations.

##### 4.2. Effects of dissolved Si and elevated pH

At pH 7 in the presence of dissolved Si, the initial  $-0.65\text{‰}$  isotopic contrast between  $\text{FeCl}_2$  and hematite moved toward the equilibrium  $\text{Fe(II)}_{\text{aq}}$ -hematite fractionation of  $-3.1\text{‰}$  (Fig. 6C and D). These data suggest a slower rate of isotopic equilibration between  $\text{Fe(II)}_{\text{aq}}$  and  $\text{Fe(III)}_{\text{reac}}$  in the presence of dissolved Si at neutral pH. Surface complexation modeling has shown that Si species bind directly to iron oxide surfaces through inner-sphere complexes (Sigg and Stumm, 1981; Barrow and Bowden, 1987), and thus may retard isotopic exchange rates. The effects of Si binding may explain the

Table 3  
 Reactive Fe species and calculated Fe isotope fractions for interactions between aqueous Fe(II) and hematite.<sup>a</sup>

Day	Fe(II) <sub>aq</sub> (mM)	Fe(II) <sub>sorb</sub> (mM)	Fe(III) <sub>reac</sub> <sup>b</sup> (mM)	Tot Reac Fe pool <sup>c</sup> (mM)	X- Fe(II) <sub>aq</sub> <sup>d</sup>	X- Fe(II) <sub>sorb</sub>	X- Fe(III) <sub>reac</sub>	$\Delta\text{Fe(II)}_{\text{aq}}^-$ Fe(II) <sub>sorb</sub>	2 $\sigma$ error <sup>c</sup>	$\Delta\text{Fe(II)}_{\text{aq}}^-$ Fe(II) <sub>reac</sub>	2 $\sigma$ error
<b>Exp 1A</b> (pH 7, no Si, 1× agitation)											
8	0.322	0.171	0.455	0.948	0.34	0.18	0.48	-0.52	0.08	-2.69	0.11
13	0.299	0.160	0.439	0.898	0.33	0.18	0.49	-0.59	0.08	-2.84	0.11
20	0.311	0.162	0.468	0.940	0.33	0.17	0.50	-0.66	0.08	-2.89	0.11
<b>Exp 1B</b> (pH 7, no Si, constant agitation)											
8	0.292	0.150	0.543	0.985	0.30	0.15	0.55	-0.58	0.08	-2.77	0.11
13	0.267	0.157	0.524	0.948	0.28	0.17	0.55	-0.65	0.08	-2.87	0.11
20	0.263	0.146	0.471	0.879	0.30	0.17	0.54	-0.62	0.08	-2.96	0.12
<b>Exp 1C</b> (pH 7, no Si, constant agitation, variable Fe(II)/hematite ratios)											
<i>Fe(II):hematite = 0.5 mM:5 mM</i>											
4	0.498	0.018	–	–	–	–	–	-0.18	0.11	–	–
8	0.460	0.017	0.223	0.701	0.66	0.02	0.32	-0.23	0.11	-1.48	0.18
12	0.512	0.017	0.145	0.674	0.76	0.03	0.21	-0.25	0.11	-1.66	0.27
<i>Fe(II):hematite = 0.5 mM:25 mM</i>											
4	0.427	0.070	–	–	–	–	–	-0.70	0.11	–	–
8	0.390	0.050	0.395	0.835	0.47	0.06	0.47	-0.47	0.11	-2.33	0.22
12	0.416	0.062	0.373	0.851	0.49	0.07	0.44	-0.53	0.11	-2.34	0.21
<i>Fe(II):hematite = 0.5 mM:50 mM</i>											
4	0.359	0.122	0.373	0.854	0.42	0.14	0.44	-0.50	0.11	-2.80	0.46
8	0.347	0.112	0.542	1.000	0.35	0.11	0.54	-0.70	0.11	-2.83	0.18
12	0.345	0.119	0.381	0.844	0.41	0.14	0.45	-0.64	0.11	-3.11	0.50
<i>Fe(II):hematite = 0.3 mM:50 mM</i>											
4	0.235	0.115	0.547	0.896	0.26	0.13	0.61	-0.71	0.11	-2.59	0.14
8	0.143	0.108	0.329	0.580	0.25	0.19	0.57	-0.51	0.11	-2.78	0.27
12	0.170	0.096	0.287	0.553	0.31	0.17	0.52	-0.68	0.11	-3.15	0.20
<i>Fe(II):hematite = 0.1 mM: 50 mM</i>											
4	0.043	0.067	0.293	0.403	0.11	0.17	0.73	-0.58	0.11	-2.57	0.14
8	0.032	0.062	0.355	0.448	0.07	0.14	0.79	-0.56	0.11	-2.50	0.22
12	0.033	0.063	0.182	0.278	0.12	0.23	0.65	-0.66	0.11	-2.82	0.14
<b>Exp 2A</b> (pH 7, Si added, 1× agitation)											
8	0.315	0.181	0.294	0.790	0.40	0.23	0.37	-0.29	0.08	-2.22	0.24
13	0.303	0.189	0.238	0.729	0.42	0.26	0.33	-0.45	0.08	-2.73	0.31
20	0.325	0.206	0.202	0.733	0.44	0.28	0.28	-0.49	0.08	-3.21	0.50
<b>Exp 2B</b> (pH 7, Si added, constant agitation)											
8	0.285	0.170	0.374	0.829	0.34	0.20	0.45	-0.43	0.08	-2.40	0.18

(continued on next page)

Table 3 (continued)

Day	Fe(II) <sub>aq</sub> (mM)	Fe(II) <sub>sorb</sub> (mM)	Fe(III) <sub>reac</sub> <sup>b</sup> (mM)	Tot Reac Fe pool <sup>c</sup> (mM)	X- Fe(II) <sub>aq</sub> <sup>d</sup>	X- Fe(II) <sub>sorb</sub>	X- Fe(III) <sub>reac</sub>	$\Delta\text{Fe(II)}_{\text{aq}} - \text{Fe(II)}_{\text{sorb}}$	2 $\sigma$ error <sup>e</sup>	$\Delta\text{Fe(II)}_{\text{aq}} - \text{Fe(II)}_{\text{reac}}$	2 $\sigma$ error
13	0.277	0.172	0.235	0.683	0.40	0.25	0.34	-0.55	0.08	-3.05	0.37
20	0.296	0.193	0.193	0.682	0.43	0.28	0.28	-0.54	0.08	-3.49	0.49
<b>Exp 3A</b> (pH 8.7, no Si, 1× agitation)											
8	0.075	0.344	0.260	0.678	0.11	0.51	0.38	-0.36	0.08	-2.51	0.14
13	0.060	0.347	0.286	0.693	0.09	0.50	0.41	-0.53	0.08	-2.76	0.14
20	0.088	0.355	0.213	0.656	0.13	0.54	0.33	-0.46	0.08	-3.17	0.23
<b>Exp 3B</b> (pH 8.7, no Si, constant agitation)											
8	0.070	0.366	0.202	0.638	0.11	0.57	0.32	-0.46	0.08	-2.98	0.20
13	0.056	0.350	0.307	0.713	0.08	0.49	0.43	-0.51	0.08	-2.88	0.15
20	0.072	0.342	0.210	0.624	0.12	0.55	0.34	-0.52	0.08	-3.41	0.28
<b>Exp 4A</b> (pH 8.7, Si added, 1× agitation)											
8	0.025	0.374	0.077	0.476	0.05	0.78	0.16	0.02	0.12	-2.50	0.48
13	0.017	0.413	0.123	0.554	0.03	0.75	0.22	-0.36	0.12	-2.50	0.29
20	0.014	0.405	0.209	0.628	0.02	0.64	0.33	0.05	0.12	-1.58	0.20
<b>Exp 4B</b> (pH 8.7, Si added, constant agitation)											
8	0.025	0.330	0.071	0.426	0.06	0.77	0.17	-0.30	0.12	-3.80	0.90
13	0.016	0.373	0.156	0.546	0.03	0.68	0.29	-0.44	0.12	-2.49	0.28
20	0.014	0.348	0.262	0.624	0.02	0.56	0.42	-0.21	0.12	-2.14	0.20

<sup>a</sup> Fe(II)/hematite ratio is 0.5 mM:50 mM for all experiments except Exp 1C.

<sup>b</sup> see text for details about calculation of Fe(III)<sub>reac</sub> concentrations.

<sup>c</sup> Tot Reac Fe pool is the total reactive Fe pool, based on the components that were open to isotopic exchange: Fe(II)<sub>aq</sub> + Fe(II)<sub>sorb</sub> + Fe(III)<sub>reac</sub>.

<sup>d</sup> x is the mole fraction of each component out of the total reactive Fe pool.

<sup>e</sup> 2 $\sigma$  errors were generated by the Excel add-in Isoplot, based on uncertainties in isotopic measurements and the fraction of Fe(II) in the 0.5 M HCl extractions.

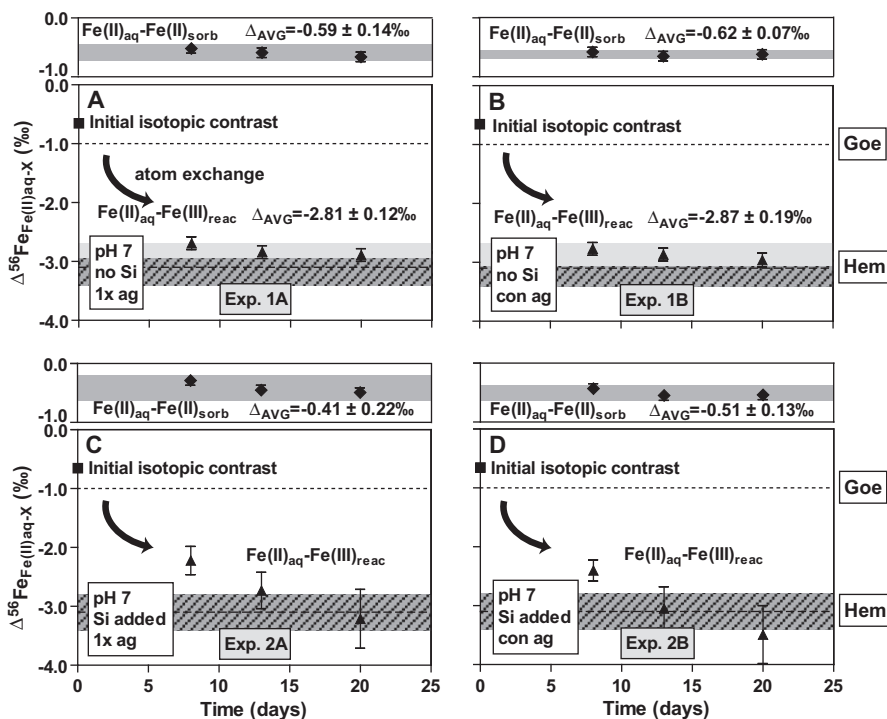


Fig. 6. Temporal variations in  $\text{Fe(II)}_{\text{aq}}\text{-Fe(II)}_{\text{sorb}}$  (◆) and  $\text{Fe(II)}_{\text{aq}}\text{-Fe(III)}_{\text{reac}}$  (▲) isotope fractionation factors for pH 7 experiments. Error bars for each time point reflect  $2\sigma$  uncertainties propagated from errors in measured  $\delta^{56}\text{Fe}$  values for  $\text{Fe(II)}_{\text{aq}}$  and  $\text{Fe(II)}_{\text{sorb}}$ , and calculated uncertainties in  $\delta^{56}\text{Fe}_{\text{Fe(III)}_{\text{reac}}}$ . Gray horizontal bars show weighted averages for each fractionation factor. Initial isotopic contrast between  $\text{FeCl}_2$  and hematite (prior to mixing) is  $-0.65\text{‰}$ . Dashed line indicates predicted  $\Delta^{56}\text{Fe}_{\text{Fe(II)}_{\text{aq}}\text{-goethite}}$  fractionation of  $-1.0\text{‰}$  (see text). Shaded horizontal bars indicate experimentally determined  $\Delta^{56}\text{Fe}_{\text{Fe(II)}_{\text{aq}}\text{-hematite}}$  fractionation of  $-3.1 \pm 0.3\text{‰}$  (see text).

decrease in the size of the reactive Fe pool observed in the pH 7, Si-bearing experiments (see Section 3.2). That isotopic equilibrium is ultimately achieved after 20 days suggests that at neutral pH binding of Si did not significantly distort Fe–O bonding in surface hematite crystals.

At pH 8.7, in the absence of Si, the  $\Delta^{56}\text{Fe}_{\text{Fe(II)}_{\text{aq}}\text{-Fe(III)}_{\text{reac}}}$  fractionations in the  $1\times$  agitated experiments moved toward the expected equilibrium  $\text{Fe(II)}_{\text{aq}}\text{-hematite}$  fractionation, and scattered about the expected fractionation in the constantly agitated experiments (Fig. 7A and B). This behavior likely reflects rapid attainment of isotopic equilibrium in the constantly agitated experiments, which minimized formation of stagnant boundary layers at the mineral-fluid interface that may have hindered isotopic exchange with the ambient solution.

Formation of an Fe hydroxide precipitate at pH 8.7 raised the possibility that this component could affect the Fe isotope compositions of  $\text{Fe(II)}_{\text{aq}}$  and  $\text{Fe(II)}_{\text{sorb}}$ . In the pH 8.7 no Si hematite-free control experiments, the fractionation factor between  $\text{Fe(II)}_{\text{aq}}$  and precipitate averaged  $-0.30 \pm 0.13\text{‰}$  when agitated once, which was similar to the fractionation factors between  $\text{Fe(II)}_{\text{aq}}$  and residue in the bottle of  $-0.26 \pm 0.19\text{‰}$  and  $-0.30 \pm 0.22\text{‰}$  for experiments agitated once and constantly, respectively (Table EA10). This suggests that the residue attached to the bottle in the pH 8.7 no Si control experiment was probably green rust. The oxidant responsible for formation of green rust remains unknown. These results indicate that, operationally, a green rust phase will have the same isotopic composition as  $\text{Fe(II)}_{\text{sorb}}$ , and

therefore it is unlikely to affect the  $\text{Fe(II)}_{\text{aq}}\text{-Fe(III)}_{\text{reac}}$  fractionations in hematite-bearing experiments under kinetic conditions because the  $\text{Fe(II)}_{\text{aq}}\text{-Fe(II)}_{\text{sorb}}$  fractionation is small, and the proportion of  $\text{Fe(II)}_{\text{sorb}}$  is low; under equilibrium conditions, the  $\text{Fe(II)}_{\text{aq}}\text{-Fe(III)}_{\text{reac}}$  fractionation is independent of isotopic fractionations among other phases.

Experiments at pH 8.7, in the presence of Si, produced unusual results. The  $\Delta^{56}\text{Fe}_{\text{Fe(II)}_{\text{aq}}\text{-Fe(III)}_{\text{reac}}}$  was approximately  $-2.50\text{‰}$  at day 8 and day 13, and then changed to  $-1.58 \pm 0.20\text{‰}$  at day 20 when agitated once (Fig. 7); the fractionation changed from  $-3.80 \pm 0.90\text{‰}$  at day 8 to  $-2.14 \pm 0.20\text{‰}$  at day 20 when agitated constantly (Fig. 7). Aqueous speciation calculations using Geochemists' Workbench (Bethke, 2002) show that in all experiments, aqueous Fe(II) existed as  $\geq 97\%$   $\text{Fe(II)(H}_2\text{O)}_6^{2+}$  under these conditions, which indicates that differences in  $\text{Fe(II)}_{\text{aq}}\text{-Fe(III)}_{\text{reac}}$  stable Fe isotope fractionations reflect changes in the nature of  $\text{Fe(III)}_{\text{reac}}$  and not  $\text{Fe(II)}_{\text{aq}}$ . This conclusion is consistent with the relatively constant  $\text{Fe(II)}_{\text{aq}}\text{-Fe(II)}_{\text{sorb}}$  fractionations in all experiments. Formation of an Fe–Si gel will have the same isotopic effects as  $\text{Fe(II)}_{\text{sorb}}$  and have no impact on the  $\Delta^{56}\text{Fe}_{\text{Fe(II)}_{\text{aq}}\text{-Fe(III)}_{\text{reac}}}$  fractionations, as evidenced in the pH 8.7 Si added, hematite-free control experiments, where the measured fractionation factor between  $\text{Fe(II)}_{\text{aq}}$  and Fe–Si gel was indistinguishable from the average  $\Delta^{56}\text{Fe}_{\text{Fe(II)}_{\text{aq}}\text{-Fe(II)}_{\text{sorb}}}$  fractionation for all hematite-bearing experiments (Wu et al., 2009).

Stable Fe isotope fractionations reflect fundamental differences in bonding environments (Schauble, 2004), and we

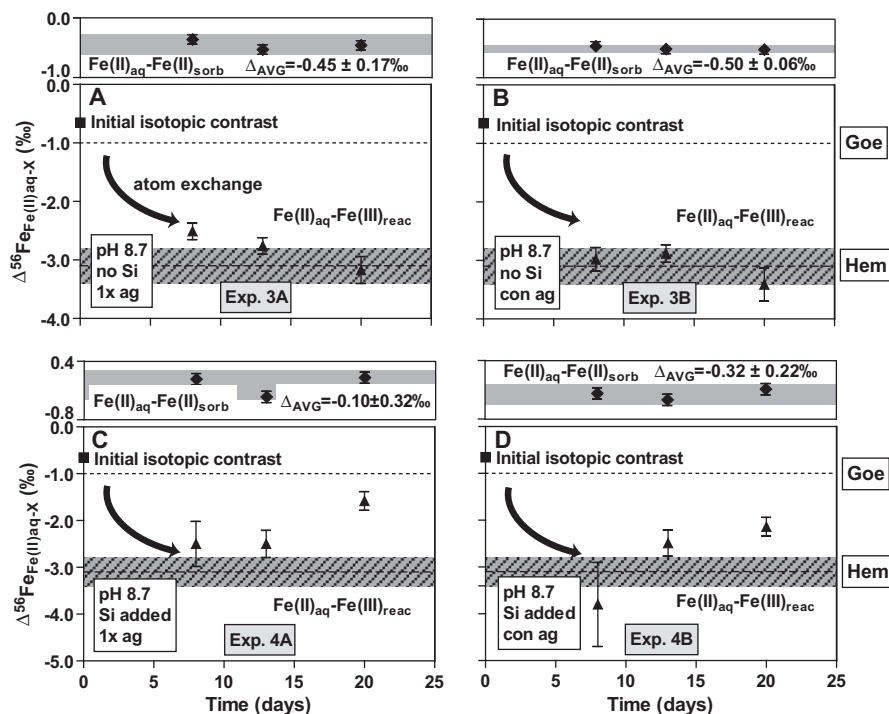


Fig. 7. Temporal variations in  $\text{Fe(II)}_{\text{aq}}\text{-Fe(II)}_{\text{sorb}}$  (◆) and  $\text{Fe(II)}_{\text{aq}}\text{-Fe(III)}_{\text{react}}$  (▲) isotope fractionation factors for experiments at pH 8.7. Error bars for each time point reflect  $2\sigma$  uncertainties propagated from errors in measured  $\delta^{56}\text{Fe}$  values for  $\text{Fe(II)}_{\text{aq}}$  and  $\text{Fe(II)}_{\text{sorb}}$ , and calculated uncertainties in  $\delta^{56}\text{Fe}_{\text{Fe(III)react}}$ . Gray horizontal bars show weighted averages for each fractionation factor. Initial isotopic contrast between  $\text{FeCl}_2$  and hematite (prior to mixing) is  $-0.65\text{‰}$ . Dashed line indicates predicted  $\Delta^{56}\text{Fe}_{\text{Fe(II)aq-goethite}}$  fractionation of  $-1.0\text{‰}$  (see text). Shaded horizontal bars indicate experimentally determined  $\Delta^{56}\text{Fe}_{\text{Fe(II)aq-hematite}}$  fractionation of  $-3.1 \pm 0.3\text{‰}$  (see text).

interpret the unusual isotopic fractionations measured in the pH 8.7, Si-bearing experiments to reflect bonding changes for Fe. Using the hematite-goethite and hematite-lepidocrocite fractionations predicted by Polyakov and Mineev (2000) and Polyakov et al. (2007), where  $\Delta^{56}\text{Fe}_{\text{hem-goe}} = +2.1\text{‰}$  and  $\Delta^{56}\text{Fe}_{\text{hem-lepid}} = +2.5\text{‰}$  at room temperature, and the experimentally determined  $\Delta^{56}\text{Fe}_{\text{Fe(II)aq-hem}}$  fractionation of  $-3.1\text{‰}$  (see previous Section 4.1), we may infer equilibrium  $\text{Fe(II)}_{\text{aq}}\text{-goethite}$  and  $\text{Fe(II)}_{\text{aq}}\text{-lepidocrocite}$  Fe isotope fractionations of  $-1.0\text{‰}$  and  $-0.6\text{‰}$ , respectively. The predicted  $\text{Fe(II)}_{\text{aq}}\text{-goethite}$  fractionation, if obtained using the difference in reduced partition function ratios between hematite and goethite, coupled to the experimentally determined  $\text{Fe(II)}_{\text{aq}}\text{-hematite}$  fractionation, has recently been experimentally confirmed (Beard et al., 2010). The distinct Fe isotope fractionations between hematite and goethite reflect the contrast in Fe bonding environments and mineral structure. In hematite, Fe is octahedrally coordinated by oxygen, with two thirds of the octahedral interstices filled with Fe(III), and layers of  $\text{FeO}_6$  octahedra are connected by edge- and face-sharing. In contrast, the goethite structure involves double bands of edge-sharing  $\text{FeO}_3(\text{OH})_3$  octahedra, where only half of the octahedral interstices are filled with Fe(III), and these are linked by corner-sharing to form tunnels crossed by hydrogen bridges, producing distinct Fe–O bond lengths relative to hematite (Blake et al., 1966; Schwertmann and Cornell, 1991). There are only small differences in Fe bonding between goethite ( $\alpha\text{-FeO}\cdot\text{OH}$ ) and lepidocrocite ( $\gamma\text{-FeO}\cdot\text{OH}$ )

(Schwertmann and Cornell, 1991), consistent with the relatively small predicted lepidocrocite-goethite stable Fe isotope fractionations.

In the presence of Si, at pH 8.7, the  $\Delta^{56}\text{Fe}_{\text{Fe(II)aq-Fe(III)react}}$  fractionation moved away from the expected  $-3.1\text{‰}$   $\text{Fe(II)}_{\text{aq}}\text{-hematite}$  fractionation and toward the  $\text{Fe(II)}_{\text{aq}}\text{-goethite}$  fractionation with time (Fig. 7C and D). This result suggests that temporal changes in Fe bonding occurred; i.e.,  $\Delta^{56}\text{Fe}_{\text{Fe(II)aq-Fe(III)react}}$  fractionations that lie between those expected for  $\text{Fe(II)}_{\text{aq}}\text{-hematite}$  and  $\text{Fe(II)}_{\text{aq}}\text{-goethite}$  may reflect distortions in Fe–O bonds. Mössbauer spectroscopy work has indicated that surface reactivity of hematite with regard to electron transfer could change over time during Fe(II) and hematite interactions (Larese-Casanova and Scherer, 2007), which is consistent with the observed temporal variation in the isotopic fractionations in our experiments.

The changes in  $\Delta^{56}\text{Fe}_{\text{Fe(II)aq-Fe(III)react}}$  fractionations may also reflect changes in Fe bonding due to surface silica species. Adsorption of Si to hematite could change the local bonding environment of reactive Fe(III) on the surface by forming Si–O–Fe bonds, and growth of Si polymers on hematite surfaces at high pH may with time distort progressively larger numbers of Fe–O bonds (Wu et al., 2009), and such a model may explain the temporal variations in  $\Delta^{56}\text{Fe}_{\text{Fe(II)aq-Fe(III)react}}$  in the pH 8.7 plus Si experiments (Fig. 7C and D). Scanning tunneling microscopy (STM) has shown that different surface sites can result in substantially different electron transfer characteristics as a result of

different solvent reorganization energies (Eggleston et al., 2004). The presence of Si polymers could potentially alter surface sites of hematite, subsequently affecting their electron transfer characteristics. This type of surface site alteration may be similar to the findings of Rea et al. (1994), who proposed that a population of labile sites that contained more distorted octahedral geometry at local environments are characteristic of the ferrihydrite surface.

#### 4.3. Number of octahedral layers involved in Fe isotope exchange

It is useful to cast the moles of the  $\text{Fe(III)}_{\text{reac}}$  component in our experiments in terms of the number of surface/near-surface octahedral layers that underwent isotopic exchange, based on the moles of the  $\text{Fe(III)}_{\text{reac}}$  component and the average diameter of the hematite crystals used in the experiments (100 nm). Cell parameters of  $a = 0.50$  nm and  $c = 1.38$  nm were used for the hematite hexagonal unit cell (Schwertmann and Cornell, 1991), and a constant density was assumed in the calculation. For the majority of the experiments, the reactive Fe(III) on the hematite surface that underwent isotopic exchange accounted for less than one octahedral layer (Figs. 8 and EA5). As greater numbers of octahedral layers on the hematite surface underwent isotopic exchange, as observed in the pH 7 no Si experiments with increasing Fe(II)/hematite ratios, as well as in the pH 8.7 plus Si experiments, the  $\Delta^{56}\text{Fe}_{\text{Fe(II)aq-Fe(III)reac}}$  fractionation moved from that expected for Fe(II)<sub>aq</sub>-hematite towards a fractionation characteristic of Fe(II)<sub>aq</sub>-goethite (Fig. 8A); these results suggest a progressive increase in the number of distorted Fe–O bonds over time.

Consideration of thermodynamic relations indicates the possibility of Fe(III) oxyhydroxide precipitation on the hematite surface in the high pH experiments, as well as experiments with high Fe(II)<sub>aq</sub>/hematite ratios. It is therefore possible that part of the  $\text{Fe(III)}_{\text{reac}}$  component may be precipitated Fe oxyhydroxide. Such precipitation could not, however, account for the transition toward Fe(II)<sub>aq</sub>-goethite fractionation factors in high pH and high Fe(II)<sub>aq</sub>/hematite experiments, based on the equilibrium  $\Delta^{56}\text{Fe}_{\text{Fe(II)aq-Ferrihydrite}}$  fractionation of  $-3.0\%$  determined by Wu et al. (2010) using the “three-isotope” method. That the  $\Delta^{56}\text{Fe}_{\text{Fe(II)aq-Fe(III)reac}}$  fractionations for the pH 8.7 plus Si experiment are distinct from those for the other two experiments which lie close to the equilibrium Fe(II)<sub>aq</sub>-hematite fractionation (Figs. 6 and 7), indicates that the presence of a Si polymer at high pH is the likely cause for the observed fractionations, reflecting stronger distortion of Fe–O bonds. In contrast, the number of octahedral layers involved was relatively constant with time for the experiments that used 0.5 mM Fe(II)<sub>aq</sub> and 50 mM hematite (Fig. 8B). In summary, our experiments have shown that different experimental conditions, including variable Fe(II)/hematite ratios, the presence of dissolved ions like Si, and/or high pH, likely changed local bonding environments of surface hematite through alteration of the amount and/or intensity of distortion of Fe–O bonds, resulting in distinct Fe(II)<sub>aq</sub>-Fe(III)<sub>reac</sub> Fe isotope fractionations. These results demonstrate that stable isotope fractionations may

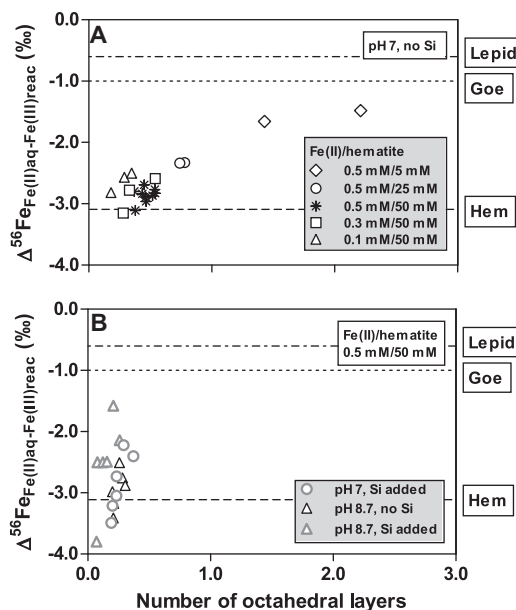


Fig. 8.  $\text{Fe(II)}_{\text{aq}}\text{-Fe(III)}_{\text{reac}}$  isotope fractionation factors versus calculated number of octahedral layers that underwent isotopic exchange for experiments at pH 7 no Si with variable Fe(II)/hematite ratios (A) and experiments at pH 7 plus Si and pH 8.7 with and without Si (B). For pH 7 no Si experiments, as more octahedral layers underwent isotopic exchange, the  $\Delta^{56}\text{Fe}_{\text{Fe(II)aq-Fe(III)reac}}$  fractionations move from that expected for hematite towards that predicted for goethite. The  $\Delta^{56}\text{Fe}_{\text{Fe(II)aq-Fe(III)reac}}$  fractionations also deviate from that expected for hematite in the presence of Si and/or at high pH, indicating formation of a new reactive Fe(III) phase other than hematite.

serve as a proxy for the changes in structure of the surface Fe oxide that undergoes electron and atom exchange after exposure to aqueous Fe(II). Moreover, these findings suggest that the Fe isotope compositions of aqueous Fe may be controlled by the isotopic properties of surface Fe during aqueous-oxide interaction, rather than the bulk mineral; the important role of surface Fe(III) in determining the Fe isotope composition of Fe(II)<sub>aq</sub> was also seen in the system Fe(II)<sub>aq</sub>-goethite (Beard et al., 2010).

#### 4.4. Implications for tracing biogeochemical cycling in the modern and ancient Earth

There is a growing body of data which indicates that negative  $\delta^{56}\text{Fe}$  values for Fe(II)<sub>aq</sub> in natural systems reflects DIR (e.g., Bergquist and Boyle, 2006; Severmann et al., 2006; Staubwasser et al., 2006; Fehr et al., 2008; Severmann et al., 2008; Homoky et al., 2009; Teutsch et al., 2009; Tangalos et al., 2010). This in turn has led workers on ancient marine sedimentary rocks to suggest that negative  $\delta^{56}\text{Fe}$  values, particularly for Fe-rich rocks, most likely reflect ancient DIR (e.g., Yamaguchi et al., 2005; Archer and Vance, 2006; Jenkyns et al., 2007; Johnson et al., 2008a,b; Severmann et al., 2008), although other workers have favored abiological processes for production of negative  $\delta^{56}\text{Fe}$  values in the ancient rock record (Rouxel et al., 2005; Anbar and Rouxel, 2007). As highlighted by Johnson et al.

(2008b), this debate centers on the quantities of low- $\delta^{56}\text{Fe}$  aqueous Fe(II) produced, where DIR, if sustained by a flux of reactive Fe(III) and organic carbon, is thought to produce greater quantities of low- $\delta^{56}\text{Fe}$  Fe(II)<sub>aq</sub> than abiogenic Fe(II) oxidation and precipitation, which produces only small quantities of Fe(II)<sub>aq</sub> that have low  $\delta^{56}\text{Fe}$  values.

Our results confirm the proposal by Crosby et al. (2007) that the mechanism for producing Fe isotope fractionation during microbial reduction of hematite lies in isotopic exchange between Fe(II)<sub>aq</sub> and reactive Fe(III) on the oxide surface. The resultant isotopic fractionations can be entirely explained by the intrinsic Fe(II)<sub>aq</sub>-oxide/hydroxide fractionations that have been measured or predicted for abiogenic systems. Crosby et al. (2007) suggested that the role of bacteria was to catalyze isotopic exchange via electron pumping to the surface of iron oxides. The results presented here, however, show that isotopic exchange may occur in abiogenic systems where Fe(II) and Fe(III) oxide are in close proximity, most likely requiring significant sorbed Fe(II). The changes in isotopic fractionations as a function of pH and dissolved silica are broadly the same for the abiogenic experiments of the current study and those produced by DIR under conditions of variable pH and dissolved silica (Wu et al., 2009). In light of these results, it may be logical to ask, “can Fe isotopes be used to distinguish biological and abiogenic processes?”

For Fe(II)<sub>aq</sub> – oxide interactions that involve hematite, our results indicate that isotopic exchange is limited to one or two surface layers of octahedra, consistent with the  $^{55}\text{Fe}$  tracer experiments of Pedersen et al. (2005), which showed extremely limited exchange. In an abiogenic system where Fe(II)<sub>aq</sub> and hematite interact, the changes in  $\delta^{56}\text{Fe}$  values for Fe(II)<sub>aq</sub> that would result from atom and electron exchange will be determined by the molar ratio of Fe(II)<sub>aq</sub> and hematite, specifically surface Fe(III) on hematite. At the low ratios used in the current study (generally 1:100 Fe(II)<sub>aq</sub>:hematite), the isotopic shifts for Fe(II)<sub>aq</sub> will be relatively large. If, however, in an abiogenic system, the proportions of Fe(II)<sub>aq</sub> and hematite remain unchanged, only relatively small quantities of low- $\delta^{56}\text{Fe}$  Fe(II)<sub>aq</sub> will be produced through coupled atom and electron exchange, where the decrease in  $\delta^{56}\text{Fe}$  will be greatest at very low Fe(II)<sub>aq</sub>:hematite ratios. In an open abiogenic system, such as that involving flow of large quantities of Fe(II)<sub>aq</sub> through a ferric oxide/hydroxide matrix, the  $\delta^{56}\text{Fe}$  values for Fe(II)<sub>aq</sub> will initially decrease but then recover to be equal to the isotopic composition of the input Fe(II)<sub>aq</sub>, as shown by the Fe(II)<sub>aq</sub>-goethite flow-through experiments of Mikutta et al. (2009).

In contrast, during DIR, new surface layers of hematite are continually exposed due to net reduction and generation of Fe(II)<sub>aq</sub>. The results presented here demonstrate that these surfaces, and the generated Fe(II)<sub>aq</sub>, will undergo isotopic exchange on timescales of days. In a closed-system, microbial hematite reduction does not run to completion due to eventual inhibition by sorbed Fe(II) (e.g., Urrutia et al., 1998; Roden and Urrutia, 1999; 2002; Roden, 2004), but if DIR-generated Fe(II)<sub>aq</sub> is advected away, DIR is a very efficient pump for producing large quantities of low- $\delta^{56}\text{Fe}$  aqueous Fe(II). Although isotopic mass balance requires that

the aqueous Fe(II) released in such an open reaction system would become less negative with increasing extent of reduction, significant amounts of low- $\delta^{56}\text{Fe}$  aqueous Fe(II) could nevertheless be generated during partial Fe(III) oxide reduction. In addition, if continued input of Fe(III) oxide (i.e. fresh Fe(III)<sub>reac</sub>) and organic matter occurs, as in modern marine sediments, production and export of low- $\delta^{56}\text{Fe}$  aqueous Fe(II) via partial Fe(III) oxide reduction and Fe isotopic exchange could be sustained indefinitely.

Full application of these results to tracing biological and abiogenic Fe redox cycling in modern or ancient natural environments requires consideration of additional factors. First, it must be recognized that hematite, although attractive experimentally because it is amenable to acid leaching, is not the most important Fe(III) oxide in most low-temperature aqueous environments. Although reaction of Fe(II)<sub>aq</sub> with poorly crystalline Fe(III)-hydroxides such as ferrihydrite rapidly produces mixed Fe(II)-Fe(III) oxides, reflecting high apparent rates of Fe isotope exchange (Pedersen et al., 2005), Fe isotope exchange rates between Fe(II)<sub>aq</sub> and ferrihydrite can be markedly decreased in complex solutions (Jones et al., 2009; Wu et al., 2010). Our full understanding of Fe isotope exchange kinetics in systems analogous to nature therefore remains incomplete. Second, prediction of the Fe isotope variations expected in natural systems requires assessment of the relative fluxes of different Fe species (Fe(II)<sub>aq</sub>, oxides, hydroxides) and basin-scale modeling. In conditions of low Fe(II)<sub>aq</sub> contents, such as in modern seawater, or hypothesized for the photic zone in the Neoproterozoic and Paleoproterozoic oceans, abiogenic Fe(II)<sub>aq</sub>-oxide Fe isotope exchange could indeed produce low  $\delta^{56}\text{Fe}$  values for Fe(II)<sub>aq</sub> in a manner similar to that produced by abiogenic Fe(II) oxidation (e.g., Bullen et al., 2001; Rouxel et al., 2005); such a record would most likely be preserved in Fe-poor rocks such as Ca–Mg carbonates. Abiogenic Fe(II) oxidation, or abiogenic Fe(II)<sub>aq</sub>-oxide interaction, however, cannot explain the low  $\delta^{56}\text{Fe}$  values found in Fe-rich marine sedimentary rocks, because these require mobilization of large quantities of low- $\delta^{56}\text{Fe}$  Fe(II)<sub>aq</sub> (e.g., Johnson et al., 2008b). Abiogenic Fe(II)<sub>aq</sub>-oxide interaction, at high Fe(II)<sub>aq</sub>:oxide ratios, will not produce low  $\delta^{56}\text{Fe}$  values for Fe(II)<sub>aq</sub>. Similarly, extensive oxidation of Fe(II) produces low  $\delta^{56}\text{Fe}$  values in the remaining Fe(II)<sub>aq</sub> only after large extents of oxidation, where the quantities of Fe(II)<sub>aq</sub> are very low. It is, therefore, not sufficient to consider only the  $\delta^{56}\text{Fe}$  values for modern or ancient natural systems when evaluating the role of abiogenic or biogenic processes, but the depositional and mass-balance constraints and potential Fe pathways of the specific settings also need to be taken into account.

## 5. CONCLUSIONS

Iron isotope fractionations among aqueous Fe(II) and Fe(III) oxide surface atoms (Fe(III)<sub>reac</sub>) provide insight into changes in the surface structure of hematite during interaction with aqueous Fe(II), under conditions of variable Fe(II)/hematite ratios, the presence/absence of dissolved Si, and neutral versus alkaline pH. The  $\Delta^{56}\text{Fe}_{\text{Fe(II)aq}-\text{Fe(III)reac}}$  fractionations in the absence of Si at neutral pH lie within the

0.3‰ uncertainty of the experimentally determined equilibrium  $\Delta_{\text{Fe(II)aq-hem}}^{56}\text{Fe}$  fractionation of  $-3.1\text{‰}$  (Skulan et al., 2002; Welch et al., 2003), clearly demonstrating that isotopic (atom) exchange occurred between Fe(II)<sub>aq</sub> and the surface Fe atoms on the hematite crystals. These findings confirm the coupled electron and atom exchange mechanism proposed to explain the Fe isotope fractionations produced during microbial hematite reduction (Crosby et al., 2005, 2007). In the presence of dissolved Si at high pH or with higher Fe(II)/hematite molar ratios, the  $\Delta_{\text{Fe(II)aq-Fe(III)reac}}^{56}\text{Fe}$  fractionation often deviated from the expected  $-3.1\text{‰}$  Fe(II)<sub>aq</sub>-hematite fractionation and moved towards those expected for aqueous Fe(II) and goethite, suggesting formation of new phases on the hematite surface as a result of distortion of near-surface Fe–O bonds and Si polymerization at high pH. In addition, high pH and the presence of Si appears to slow the rate of isotopic exchange between Fe(II)<sub>aq</sub> and Fe(III)<sub>reac</sub>. Surface phase alteration may have important implications for the reducibility of Fe(III) oxides by dissimilatory iron-reducing bacteria (e.g., Cutting et al., 2009), as well as the reactivity of aqueous Fe(II) when interacting with contaminants in the presence of oxide surfaces (Buerge and Hug, 1999; Elsner et al., 2004b).

As suggested by numerous studies of Fe isotopes in natural environments (e.g., Bergquist and Boyle, 2006; Severmann et al., 2006; Staubwasser et al., 2006; Fehr et al., 2008; Severmann et al., 2008; Homoky et al., 2009; Teutsch et al., 2009; Tangalos et al., 2010), dissimilatory microbial iron reduction (DIR) remains the most likely process for producing large quantities of aqueous Fe(II) that has low  $\delta^{56}\text{Fe}$  values. Although abiogenic Fe(II)<sub>aq</sub>-oxide interactions, as studied here, may produce low  $\delta^{56}\text{Fe}$  values similar to those produced by abiogenic oxidation of Fe(II), this only occurs at low Fe(II)<sub>aq</sub>/oxide ratios. DIR, on the other hand, continually exposes new surface Fe(III) layers, which, along with production of Fe(II), suggests that DIR is a more efficient “pump” for producing large quantities of low- $\delta^{56}\text{Fe}$  Fe(II)<sub>aq</sub> than abiogenic Fe(II) oxidation or Fe(II)<sub>aq</sub>-oxide interaction.

#### ACKNOWLEDGEMENTS

This research was supported by NSF Grant 0525417, as well as the NASA Astrobiology Institute. Huifang Xu is thanked for helping with calculation of octahedral layers. Comments by two anonymous reviewers and A.E. Rehkämper, helped to improve the manuscript.

#### APPENDIX A. SUPPLEMENTARY DATA

Supplementary data associated with this article can be found, in the online version, at doi:10.1016/j.gca.2010.04.060.

#### REFERENCES

- Anbar A. D., Jarzecki A. A. and Spiro T. G. (2005) Theoretical investigation of iron isotope fractionation between  $\text{Fe}(\text{H}_2\text{O})_6^{3+}$  and  $\text{Fe}(\text{H}_2\text{O})_6^{2+}$ : implications for iron stable isotope geochemistry. *Geochim. Cosmochim. Acta* **69**, 825–837.
- Anbar A. D. and Rouxel O. (2007) Metal stable isotopes in paleoceanography. *Annu. Rev. Earth Pl. Sc.* **35**, 717–746.
- Archer C. and Vance D. (2006) Coupled Fe and S isotope evidence for Archean microbial Fe(III) and sulfate reduction. *Geology* **34**, 153–156.
- Barrow N. J. and Bowden J. W. (1987) A comparison of models for describing the adsorption of anions A on a variable charge mineral surface. *J. Colloid Interface Sci.* **119**, 236–250.
- Beard, B. L., Handler, R., Scherer, M. M., Wu, L., Czaja, A., Heimann, A. and Johnson, C. M. (2010) Iron isotope fractionation between aqueous ferrous iron and goethite. *Earth Planet. Sci. Lett.*, doi:10.1016/j.epsl.2010.04.006.
- Beard, B. L., Johnson, C. M., Cox, L., Sun, H. and Nealon, K. H. (1999) Iron isotope biosignatures. *Science* **285**.
- Beard B. L., Johnson C. M., Skulan J. L., Nealon K. H., Cox L. and Sun H. (2003) Application of Fe isotopes to tracing the geochemical and biological cycling of Fe. *Chem. Geol.* **195**, 87–117.
- Bergquist B. A. and Boyle E. A. (2006) Iron isotopes in the Amazon River system: weathering and transport signatures. *Earth Planet. Sci. Lett.* **248**, 54–68.
- Bethke C. M. (2002) *The Geochemist's Workbench 4.0*. Urbana, IL.
- Blake R. L., Hessevick R. E., Zoltai T. and Finger L. W. (1966) Refinement of hematite structure. *Am. Mineral.* **51**, 123–129.
- Blanchard M., Poitrasson F., Méheut M., Lazzeri M., Mauri F. and Balan E. (2009) Iron isotope fractionation between pyrite (FeS<sub>2</sub>), hematite (Fe<sub>2</sub>O<sub>3</sub>) and siderite (FeCO<sub>3</sub>): a first-principles density functional theory study. *Geochim. Cosmochim. Acta* **73**, 6565–6578.
- Buerge I. J. and Hug S. J. (1999) Influence of mineral surfaces on chromium(VI) reduction by iron(II). *Environ. Sci. Technol.* **33**, 4285–4291.
- Bullen T. D., White A. F., Childs C. W., Vivit D. V. and Schulz M. S. (2001) Demonstration of significant abiotic iron isotope fractionation in nature. *Geology* **29**, 699–702.
- Crosby H. A., Johnson C. M., Roden E. E. and Beard B. L. (2005) Coupled Fe(II)–Fe(III) electron and atom exchange as a mechanism for Fe isotope fractionation during dissimilatory iron oxide reduction. *Environ. Sci. Technol.* **39**, 6698–6704.
- Crosby, H. A., Roden, E. E., Johnson, C. M. and Beard, B. L. (2007). The mechanisms of iron isotope fractionation produced during dissimilatory Fe(III) reduction by *Shewanella putrefaciens* and *Geobacter sulfurreducens*. *Geobiology*, doi:10.1111/j.1472-4669.2007.00103.x.
- Cutting R. S., Coker V. S., Fellowes J. W., Lloyd J. R. and Vaughan D. J. (2009) Mineralogical and morphological constraints on the reduction of Fe(III) minerals by *Geobacter sulfurreducens*. *Geochim. Cosmochim. Acta* **73**, 4004–4022.
- Eggleston C. M., Stack A. G., Rosso K. M. and Bice A. M. (2004) Adatom Fe(III) on the hematite surface: observation of a key reactive surface species. *Geochem. Trans.* **5**, 33–40.
- Eggleston C. M., Stack A. G., Rosso K. M., Higgins S. R., Bice A. M., Boese S. W., Pribyl R. D. and Nichols J. J. (2003) The structure of hematite ( $\alpha\text{-Fe}_2\text{O}_3$ ) (0 0 1) surfaces in aqueous media: scanning tunneling microscopy and resonant tunneling calculations of coexisting O and Fe terminations. *Geochim. Cosmochim. Acta* **67**, 985–1000.
- Elsner M., Haderlein S. B., Kellerhals T., Luzi S., Zwank L., Angst W. and Schwarzenbach R. P. (2004a) Mechanisms and products of surface-mediated reductive dehalogenation of carbon tetrachloride by Fe(II) on goethite. *Environ. Sci. Technol.* **38**, 2058–2066.
- Elsner M., Schwarzenbach R. P. and Haderlein S. B. (2004b) Reactivity of Fe(II)-bearing minerals toward reductive transformation of organic contaminants. *Environ. Sci. Technol.* **38**, 799–807.

- Fehr M. A., Andersson P. S., Hälenius U. and Mörrh C.-M. (2008) Iron isotope variations in Holocene sediments of the Gotland Deep, Baltic Sea. *Geochim. Cosmochim. Acta* **72**, 807–826.
- Fredrickson J. K. and Gorby Y. A. (1996) Environmental processes mediated by iron-reducing bacteria. *Curr. Opin. Biotechnol.* **7**, 287–294.
- Handler R., Beard B. L., Johnson C. M. and Scherer M. M. (2009) Atom exchange between aqueous Fe(II) and goethite: an Fe isotope tracer study. *Environ. Sci. Technol.* **43**, 1102–1107.
- Heijman C. G., Grieder E., Holliger C. and Schwarzenbach R. P. (1995) Reduction of nitroaromatic compounds coupled to microbial iron reduction in laboratory aquifer columns. *Environ. Sci. Technol.* **29**, 775–783.
- Heijman C. G., Holliger C., Glaus M. A., Schwarzenbach R. P. and Zeyer J. (1993) Abiotic reduction of 4-chloronitrobenzene to 4-chloroaniline in a dissimilatory iron-reducing enrichment culture. *Appl. Environ. Microbiol.* **59**, 4350–4353.
- Hiemstra T. and van Riemsdijk W. H. (2007) Adsorption and surface oxidation of Fe(II) on metal (hydr)oxides. *Geochim. Cosmochim. Acta* **71**, 5913–5933.
- Hofstetter T. B., Schwarzenbach R. P. and Haderlein S. B. (2003) Reactivity of Fe(II) species associated with clay minerals. *Environ. Sci. Technol.* **37**, 519–528.
- Homoky W. B., Severmann S., Mills R. A., Statham P. J. and Fones G. R. (2009) Pore-fluid Fe isotopes reflect the extent of benthic Fe redox recycling: evidence from continental shelf and deep-sea sediments. *Geology* **37**, 751–754.
- Icopini G. A., Anbar A. D., Ruebush S. S., Tien M. and Brantley S. L. (2004) Iron isotope fractionation during microbial reduction of iron: the importance of adsorption. *Geology* **32**, 205–208.
- Jenkyns, H., Matthews, A., Tsikos, H. and Erel, Y. (2007) Nitrate reduction, sulfate reduction and sedimentary iron-isotope evolution during the Cenomanian–Turonian Anoxic Event. *Paleoceanography* **22**, PA3208.
- Jeon B.-H., Dempsey B. A., Burgos W. D. and Royer R. A. (2001) Reactions of ferrous iron with hematite. *Colloid. Surface. A* **191**, 41–55.
- Jeon B. H., Dempsey B. A. and Burgos W. D. (2003) Kinetics and mechanisms for reactions of Fe(II) with iron(III) oxides. *Environ. Sci. Technol.* **37**, 3309–3315.
- Johnson C. M., Beard B. L., Klein C., Beukes N. J. and Roden E. E. (2008a) Iron isotopes constrain biologic and abiologic processes in banded iron formation genesis. *Geochim. Cosmochim. Acta* **72**, 151–169.
- Johnson C. M., Beard B. L. and Roden E. E. (2008b) The iron isotope fingerprints of redox and biogeochemical cycling in modern and ancient Earth. *Annual Review of Earth & Planetary Sciences* **36**, 457–493.
- Johnson C. M., Roden E. E., Welch S. A. and Beard B. L. (2005) Experimental constraints on Fe isotope fractionation during magnetite and Fe carbonate formation coupled to dissimilatory hydrous ferric oxide reduction. *Geochim. Cosmochim. Acta* **69**, 963–993.
- Jones A. M., Collins R. N., Rose J. and Waite T. D. (2009) The effect of silica and natural organic matter on the Fe(II)-catalysed transformation and reactivity of Fe(III) minerals. *Geochim. Cosmochim. Acta* **73**, 4409–4422.
- Kerisit S. and Rosso K. M. (2006) Computer simulation of electron transfer at hematite surfaces. *Geochim. Cosmochim. Acta* **70**, 1888–1903.
- Kerisit S. and Rosso K. M. (2007) Kinetic Monte Carlo model of charge transport in hematite ( $\alpha$ -Fe<sub>2</sub>O<sub>3</sub>). *J. Chem. Phys.* **127**, 124706–124710.
- Kohn T., Livi K. J. T., Roberts A. L. and Vikesland P. J. (2005) Longevity of granular iron in groundwater treatment processes: corrosion product development. *Environ. Sci. Technol.* **39**, 2867–2879.
- Konhauser K. O., Lalonde S. V., Amskold L. and Holland H. D. (2007) Was there really an Archean phosphate crisis? *Science* **315**, 1234.
- Krishnamurti G. S. R. and Huang P. M. (1990) Spectrophometric determination of Fe(II) with 2,4,6-Tri(2'-pyridyl)-1,3,5-triazine in the presence of large quantities of Fe(III) and complexing ions. *Talanta* **37**, 745–748.
- Larese-Casanova P. and Scherer M. M. (2007) Fe(II) sorption on hematite: new insights based on spectroscopic measurements. *Environ. Sci. Technol.* **41**, 471–477.
- Liger E., Charlet L. and Van Cappellen P. (1999) Surface catalysis of uranium(VI) reduction by iron(II). *Geochim. Cosmochim. Acta* **63**, 2939–2955.
- Lovley D. R. (1989) Oxidation of aromatic contaminants coupled to microbial iron reduction. *Nature* **339**, 297–300.
- Ludwig K. R. (1991) *ISOPLOT: A Plotting and Regression Program for Radiogenic-Isotope Data, Version 2.53*. US Geological Survey, Reston, VA.
- Maliva R. G., Knoll A. H. and Simonson B. M. (2005) Secular change in the Precambrian silica cycle: insights from chert petrology. *Geol. Soc. Amer. Bull.* **117**, 835–845.
- Mikutta C., Wiederhold J. G., Cirpka O. A., Hofstetter T. B., Bourdon B. and Gunten U. V. (2009) Iron isotope fractionation and atom exchange during sorption of ferrous iron to mineral surfaces. *Geochim. Cosmochim. Acta* **73**, 1795–1812.
- Mishra D. and Farrell J. (2005) Evaluation of mixed valent iron oxides as reactive adsorbents for arsenic removal. *Environ. Sci. Technol.* **39**, 9689–9694.
- Otonello G. and Zuccolini M. V. (2009) Ab-initio structure, energy and stable Fe isotope equilibrium fractionation of some geochemically relevant H–O–Fe complexes. *Geochim. Cosmochim. Acta* **73**, 6447–6469.
- Pecher K., Haderlein S. B. and Schwarzenbach R. P. (2002) Reduction of polyhalogenated methanes by surface-bound Fe(II) in aqueous suspensions of iron oxides. *Environ. Sci. Technol.* **36**, 1734–1741.
- Pedersen H. D., Postma D., Jakobsen R. and Larsen O. (2005) Fast transformation of iron oxyhydroxides by the catalytic action of aqueous Fe(II). *Geochim. Cosmochim. Acta* **69**, 3967–3977.
- Polyakov V. B., Clayton R. N., Horita J. and Mineev S. D. (2007) Equilibrium iron isotope fractionation factors of minerals: reevaluation from the data of nuclear inelastic resonant X-ray scattering and Mössbauer spectroscopy. *Geochim. Cosmochim. Acta* **71**, 3833–3846.
- Polyakov V. B. and Mineev S. D. (2000) The use of Mössbauer spectroscopy in stable isotope geochemistry. *Geochim. Cosmochim. Acta* **64**, 849–865.
- Rea B. A., Davis J. A. and Waychunas G. A. (1994) Studies of the reactivity of the ferrihydrite surface by iron isotopic exchange and Mössbauer spectroscopy. *Clay Clay Miner.* **42**, 23–34.
- Reardon E. J., Fagan R., Vogan J. L. and Przepiora A. (2008) Anaerobic corrosion reaction kinetics of nanosized iron. *Environ. Sci. Technol.* **42**, 2420–2425.
- Roden E. E. (2004) Analysis of long-term bacterial vs. chemical Fe(III) oxide reduction kinetics. *Geochim. Cosmochim. Acta* **68**, 3205–3216.
- Roden E. E. and Urrutia M. M. (1999) Ferrous iron removal promotes microbial reduction of crystalline iron(III) oxides. *Environ. Sci. Technol.* **33**, 1847–1853.
- Roden E. E. and Urrutia M. M. (2002) Influence of biogenic Fe(II) on bacterial crystalline Fe(III) oxide reduction. *Geomicrobiol. J.* **19**, 209–251.

- Rouxel O. J., Bekker A. and Edwards K. J. (2005) Iron isotope constraints on the Archean and Paleoproterozoic ocean redox state. *Science* **307**, 1088–1091.
- Rügge K., Hofstetter T. B., Haderlein S. B., Bjerg P. L., Knudsen S., Zraunig C., Mosbæk H. and Christensen T. H. (1998) Characterization of predominant reductants in an anaerobic leachate-contaminated aquifer by nitroaromatic probe compounds. *Environ. Sci. Technol.* **32**, 23–31.
- Schauble E. A. (2004) Applying stable isotope fractionation theory to new systems. *Rev. Mineral. Geochem.* **55**, 65–111.
- Schwertmann U. and Cornell R. M. (1991) *Iron Oxides in the Laboratory: Preparation and Characterization*. VCH, New York, NY.
- Severmann S., Johnson C. M., Beard B. L. and McManus J. (2006) The effect of early diagenesis on the Fe isotope compositions of porewaters and authigenic minerals in continental margin sediments. *Geochim. Cosmochim. Acta* **70**, 2006–2022.
- Severmann S., Lyons T. W., Anbar A., McManus J. and Gordon G. (2008) Modern iron isotope perspective on the benthic iron shuttle and the redox evolution of ancient oceans. *Geology* **36**, 487–490.
- Sigg L. and Stumm W. (1981) The interaction of anions and weak acids with the hydrous goethite ( $\alpha$ -FeO-OH) surface. *Colloids Surf.* **2**, 101–117.
- Silvester E., Charlet L., Tournassat C., Géhin A., Grenèche J.-M. and Liger E. (2005) Redox potential measurements and Mössbauer spectrometry of Fe<sup>II</sup> adsorbed onto Fe<sup>III</sup> (oxyhydr)oxides. *Geochim. Cosmochim. Acta* **69**, 4801–4815.
- Skulan J. L., Beard B. L. and Johnson C. M. (2002) Kinetic and equilibrium Fe isotope fractionation between aqueous Fe(III) and hematite. *Geochim. Cosmochim. Acta* **66**, 2995–3015.
- Staubwasser M., von Blanckenburg F. and Schoenberg R. (2006) Iron isotopes in the early marine diagenetic iron cycle. *Geology* **34**, 629–632.
- Stookey L. (1970) Ferrozine: a new spectrophotometric reagent for iron. *Anal. Chem.* **42**, 779–781.
- Strathmann T. J. and Stone A. T. (2003) Mineral surface catalysis of reactions between FeII and oxime carbamate pesticides. *Geochim. Cosmochim. Acta* **67**, 2775–2791.
- Tangalos, G. E., Beard, B. L., Johnson, C. M., Alpers, C. N., Shelobolina, E. S., Xu, H., Konishi, H. and Roden, E. E. (2010) Microbial production of isotopically light iron(II) in a modern chemically precipitated sediment and implications for isotopic variations in ancient rocks. *Geobiology*, doi:10.1111/j.1472-4669.2010.00237.x.
- Tanwar K. S., Petitto S. C., Ghose S. K., Eng P. J. and Trainor T. P. (2008) Structural study of Fe(II) adsorption on hematite(1102). *Geochim. Cosmochim. Acta* **72**, 3311–3325.
- Tanwar K. S., Petitto S. C., Ghose S. K., Eng P. J. and Trainor T. P. (2009) Fe(II) adsorption on hematite (0001). *Geochim. Cosmochim. Acta* **73**, 4346–4365.
- Teutsch N., Schmid M., Müller B., Halliday A. N., Bürgmann H. and Wehrli B. (2009) Large iron isotope fractionation at the oxic–anoxic boundary in Lake Nyos. *Earth Planet. Sci. Lett.* **285**, 52–60.
- Tronc E., Jolivet J.-P., Lefebvre J. and Massart R. (1984) Ion adsorption and electron transfer in spinel-like iron oxide colloids. *J. Chem. Soc., Faraday Trans. I* **80**, 2619–2629.
- Urrutia M. M., Roden E. E., Fredrickson J. K. and Zachara J. M. (1998) Microbial and geochemical controls on synthetic Fe(III) oxide reduction by *Shewanella alga* strain BrY. *Geomicrobiol. J.* **15**, 269–291.
- Vikesland P. J. and Valentine R. L. (2002) Iron oxide surface-catalyzed oxidation of ferrous iron by monochloramine: implications of oxide type and carbonate on reactivity. *Environ. Sci. Technol.* **36**, 512–519.
- Welch S. A., Beard B. L., Johnson C. M. and Braterman P. S. (2003) Kinetic and equilibrium Fe isotope fractionation between aqueous Fe(II) and Fe(III). *Geochim. Cosmochim. Acta* **67**, 4231–4250.
- Williams A. G. B. and Scherer M. M. (2004) Spectroscopic evidence for Fe(II)–Fe(III) electron transfer at the iron oxide–water interface. *Environ. Sci. Technol.* **38**, 4782–4790.
- Wu L., Beard B. L., Roden E. E. and Johnson C. M. (2009) Influence of pH and dissolved Si on Fe isotope fractionation during dissimilatory microbial reduction of hematite. *Geochim. Cosmochim. Acta* **73**, 5584–5599.
- Wu, L., Beard, B. L., Roden, E. E. and Johnson, C. M. (2010) Equilibrium iron isotope fractionation between Fe(II) and hydrous ferric oxide. *Goldschmidt 2010*. Knoxville, Tennessee.
- Yamaguchi K. E., Johnson C. M., Beard B. L. and Ohmoto H. (2005) Biogeochemical cycling of iron in the Archean–Paleoproterozoic Earth: constraints from iron isotope variations in sedimentary rocks from the Kaapvaal and Pilbara Cratons. *Chem. Geol.* **218**, 135–169.

Associate editor: Mark Rehkamper